St. Paul’s Cathedral

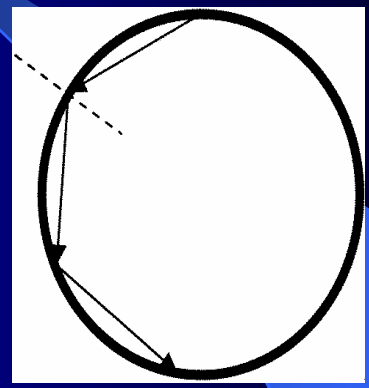

Theory of Sound

L. Rayleigh The problem of the whispering gallery, *Phil. Mag.*, **20**, 1001(1910)

Mie

Light scattering at particle with

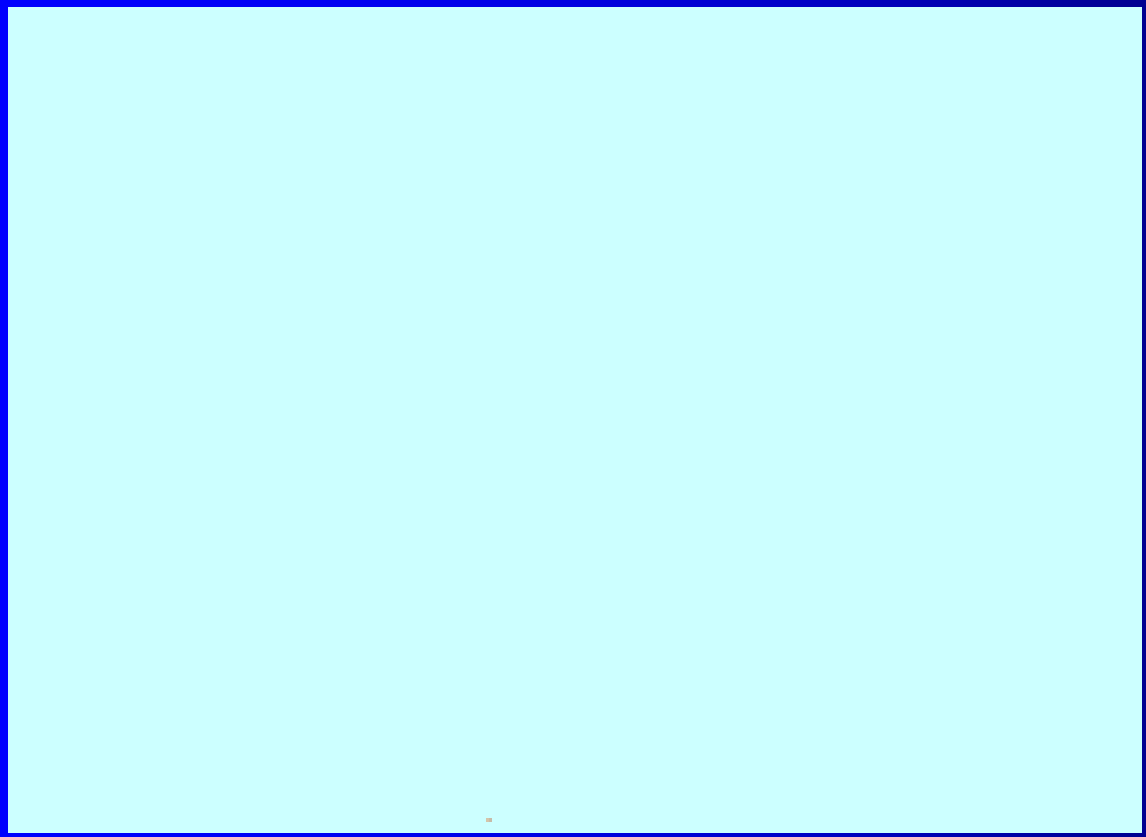

Mie G, Ann. Phys., 1908, 25(4):377

(Fabry-Pérot, FP)　　VCSEL

（Whispering-Gallery, WG)

(Photonic Crystal, PC)

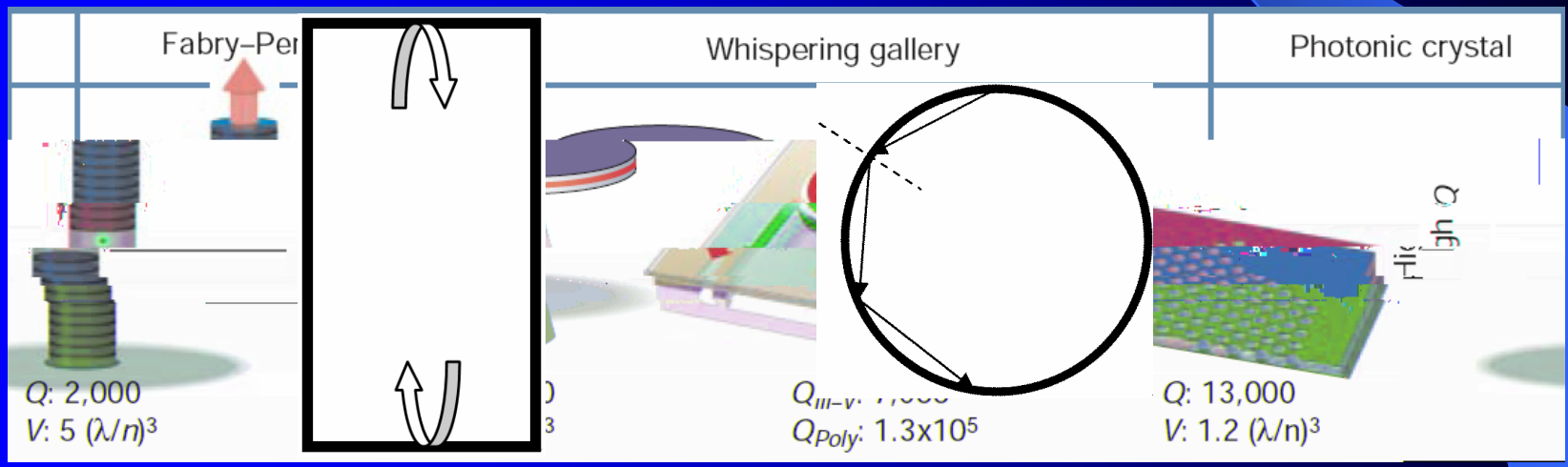

K. J. Vahala, Nature vol.424, p. 839 (2003).

Q

Q

huang4

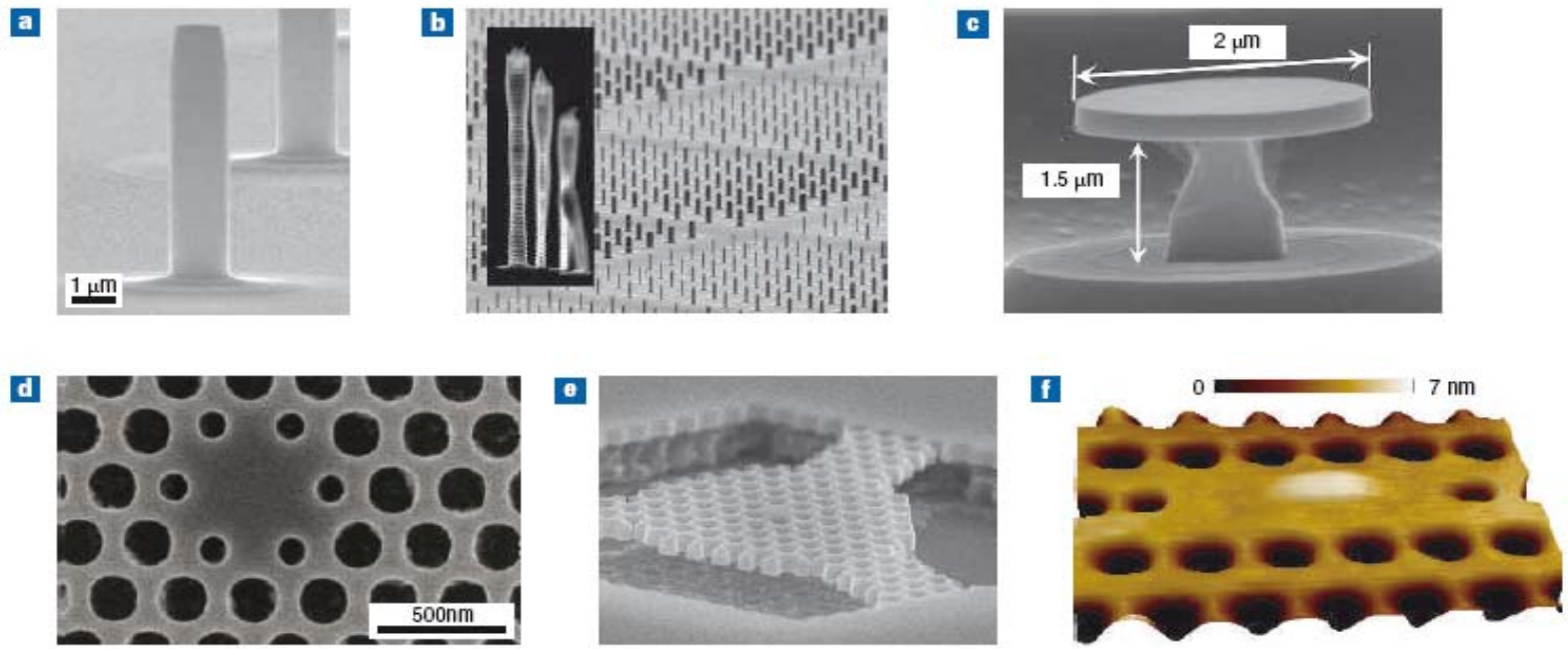

Figure 3 Scanning-electron-microscope images of semiconductor cavities. **a**,**b**, Pillar microcavities. **c**, microdisks. **d**–**f**, Photonic-bandgap defect cavities. The structures were fabricated at: **a**, University of Würzburg; **b**,**c**,**e**, CNRS-LPN (UPR-20); **d**, Univ. Cambridge; **f**, UCSB/ETHZ. (Image sources and permissions: **a**, Ref. 56. **c**, Ref. 51, copyright (2005) APS. **d**, Ref. 47, copyright (2006) AIP. **e**,**f**, Ref. 48)

huang4 yzhuang, 2008-3-6

A.

1. VCSEL

1979 InGaAsP 77K

1983 GaAs 77K

1988 850nm GaAs

1998 VCSEL

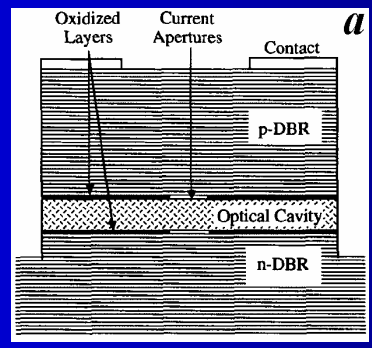

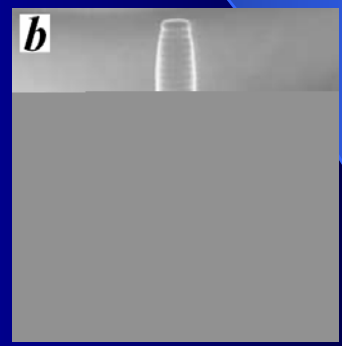

2.

1992

1992

1993

1998 150 A

2000 40 A

1.

2.

3. , ,

Whispering-Gallery Mode (WGM)

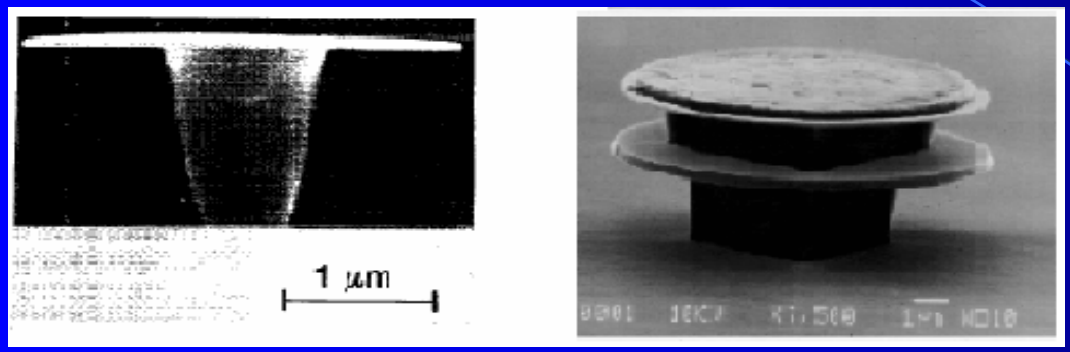

S. L. McCall et al, Appl. Phys. Lett., vol.60, 289 (1992), Electron. Lett., vol.28, p.1010(1992)

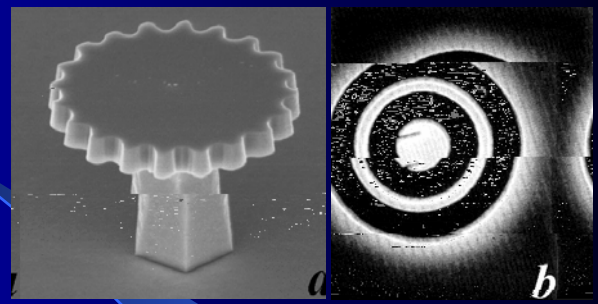

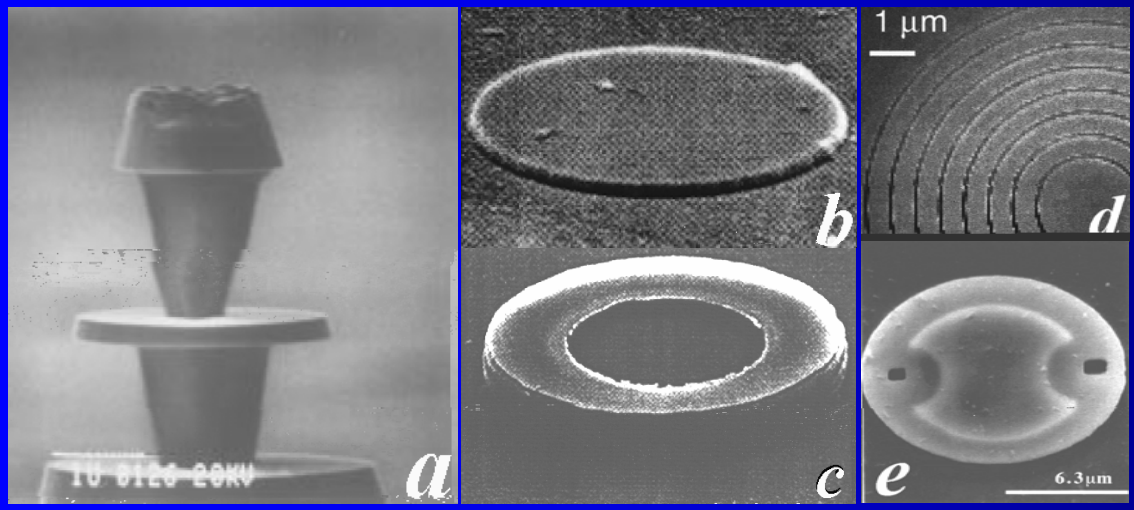

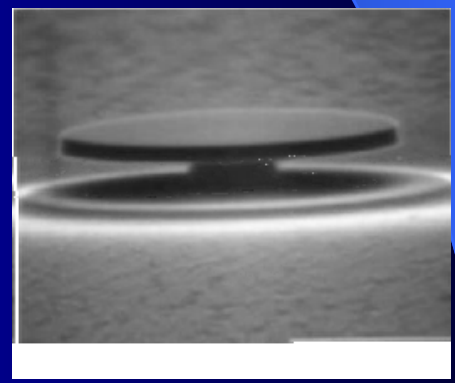

P. Michler et al, Science, vol. 290, p.2282(2000)

1999 6.75mW

2000 300μA

2004 0.25

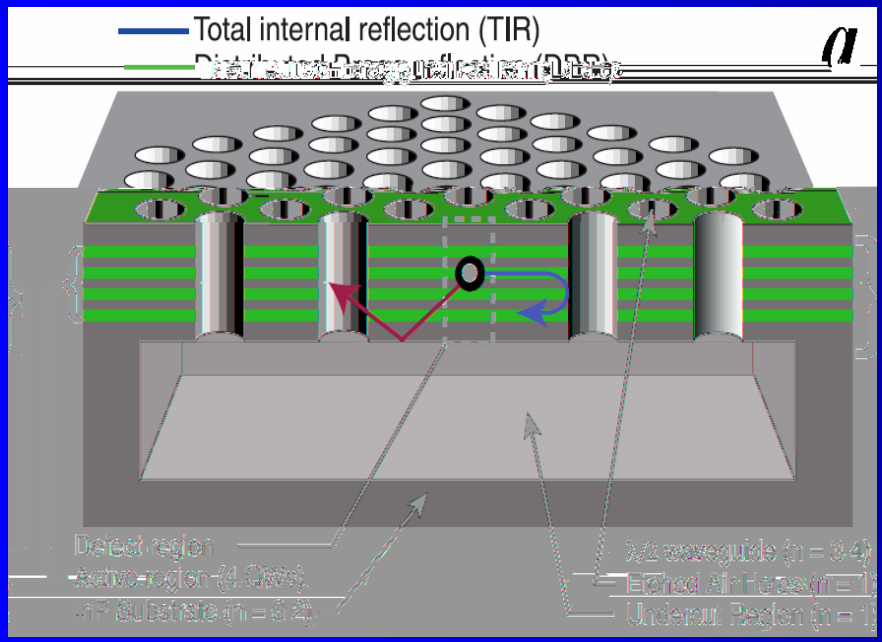

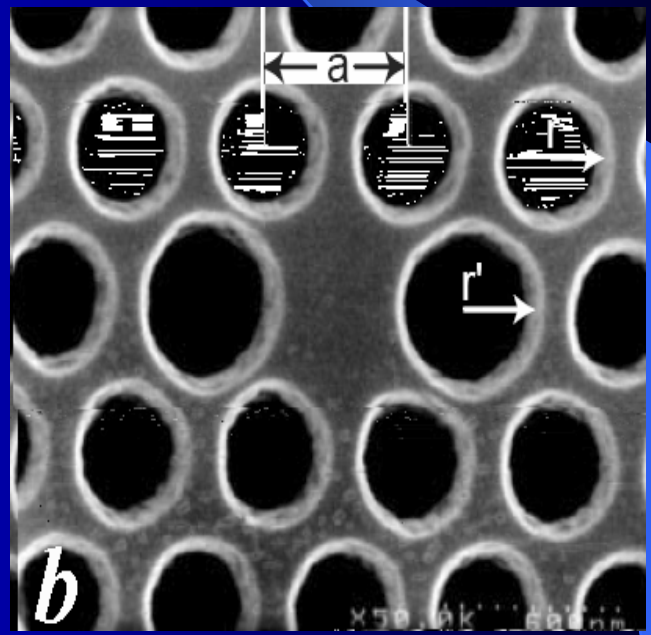

H.-G.Park, IEEE J. Quantum Electron., vol.41, p.1131(2008)

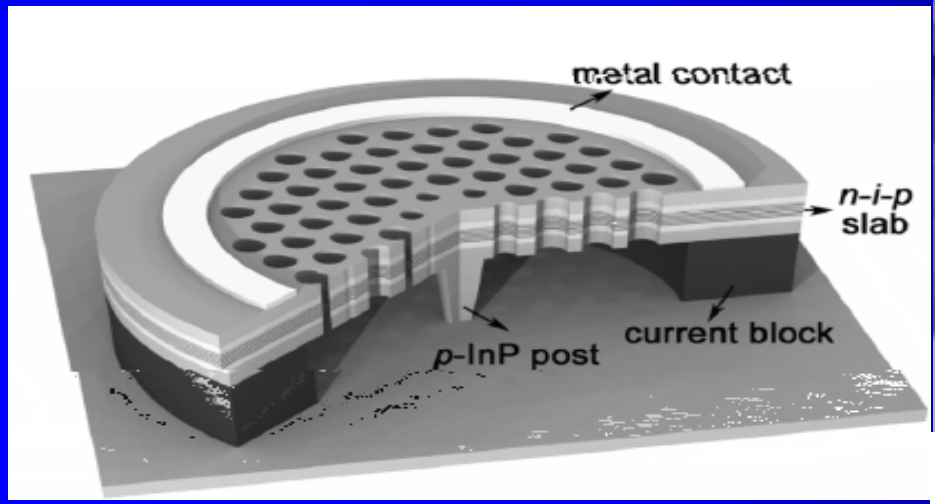

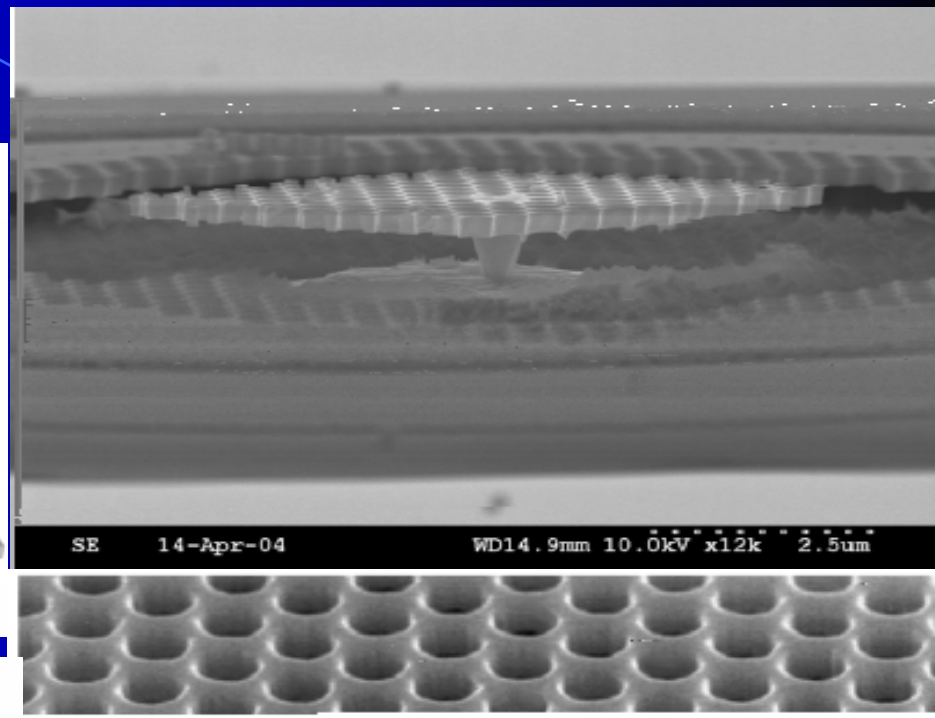

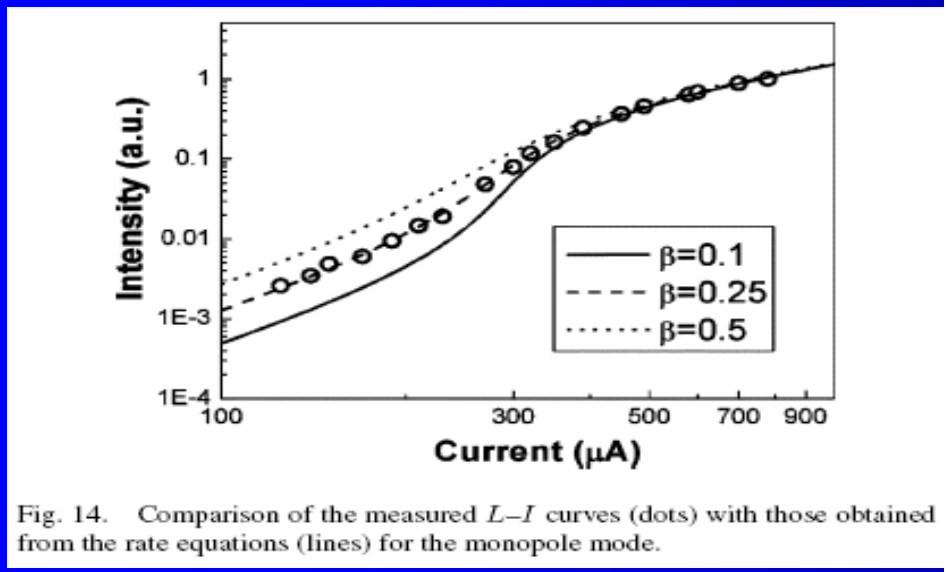

Fig. 14. Comparison of the measured L–I curves (dots) with those obtained from the rate equations (lines) for the monopole mode.

The coupling of mechanical and optical degrees of freedom via radiation pressure has been a subject of early research in the context of gravitational wave detection.

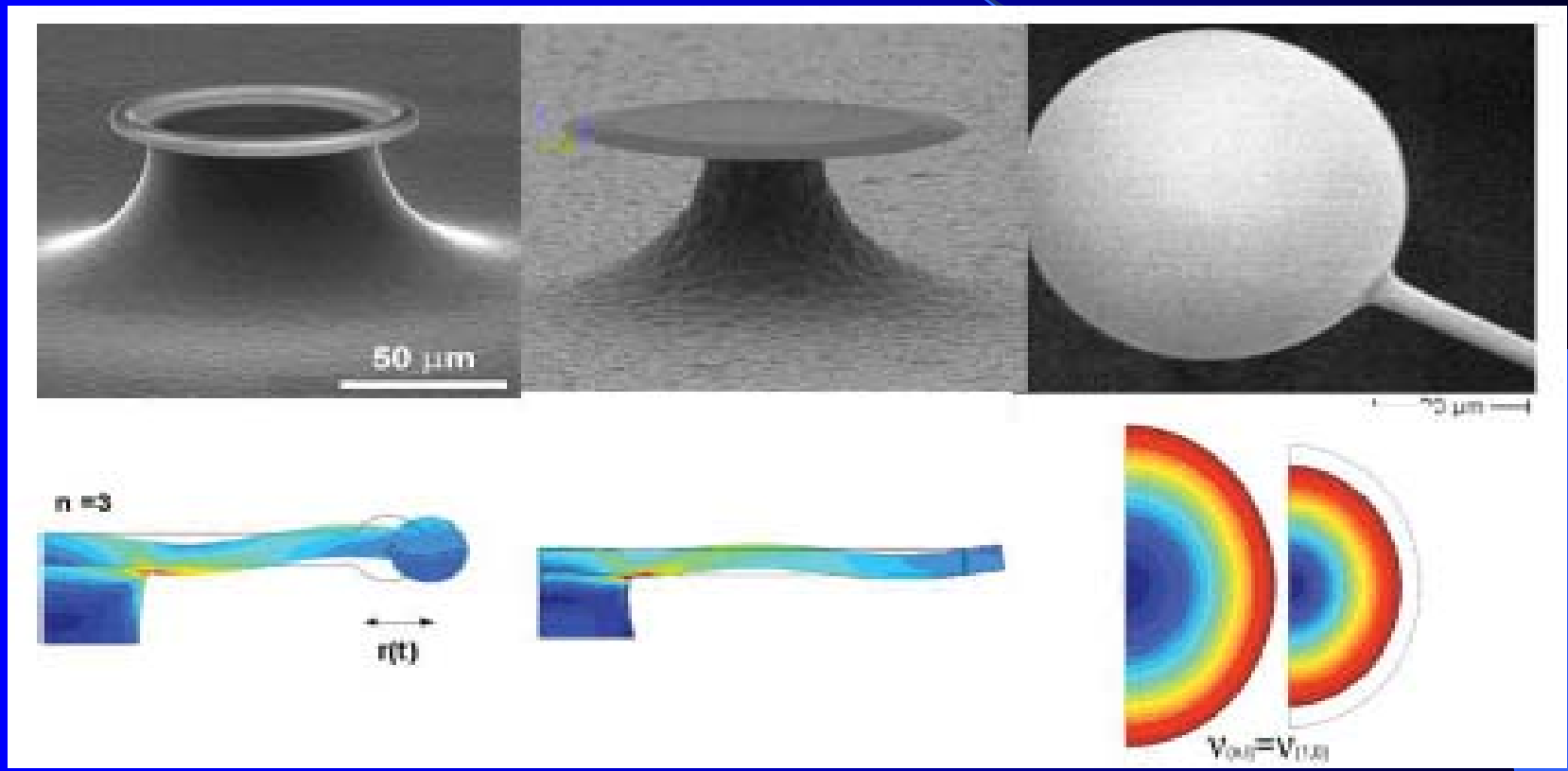

T.J. Kippenberg and K.J. Vahala, “Cavity opto-mechanics” Optics Express, vol.15, p.17172(2007)

Y. Takahashi, et al, "High-*Q* nanocavity with a 2-ns photon lifetime", Optics Express, vol.15, p.17206(2007)
corresponds to a quality factor of 2.5×10^6 ,standard deviations are less than 1 nm.

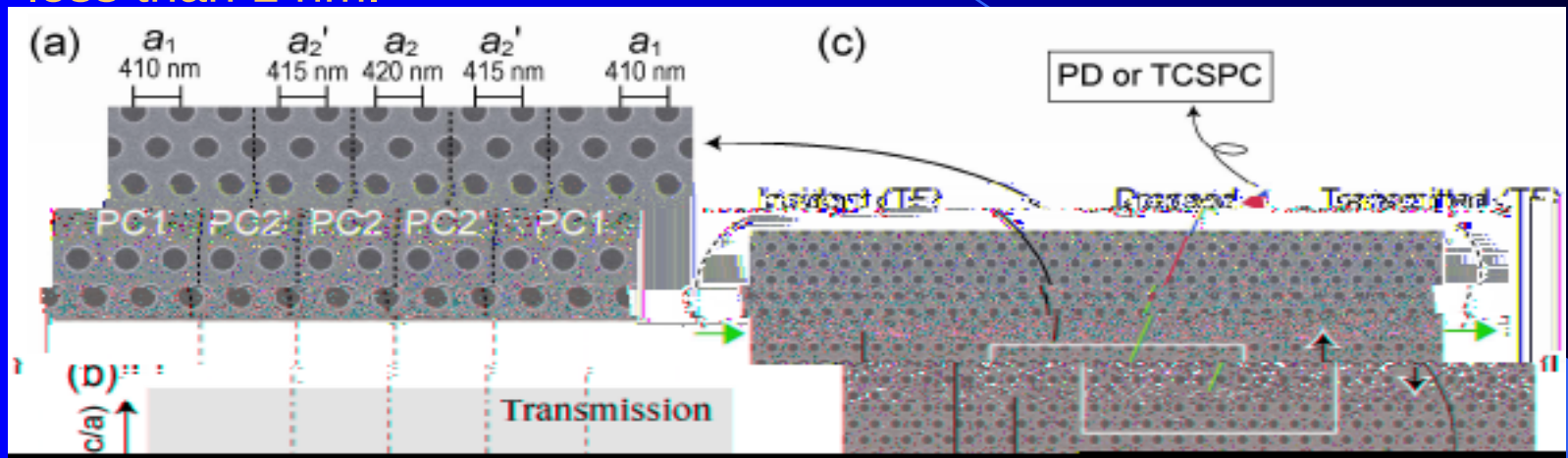

Q

K. Hennessy, et al, “Quantum nature of a strongly coupled single quantum dot–cavity system,” Nature, vol.445, p.896(2007)

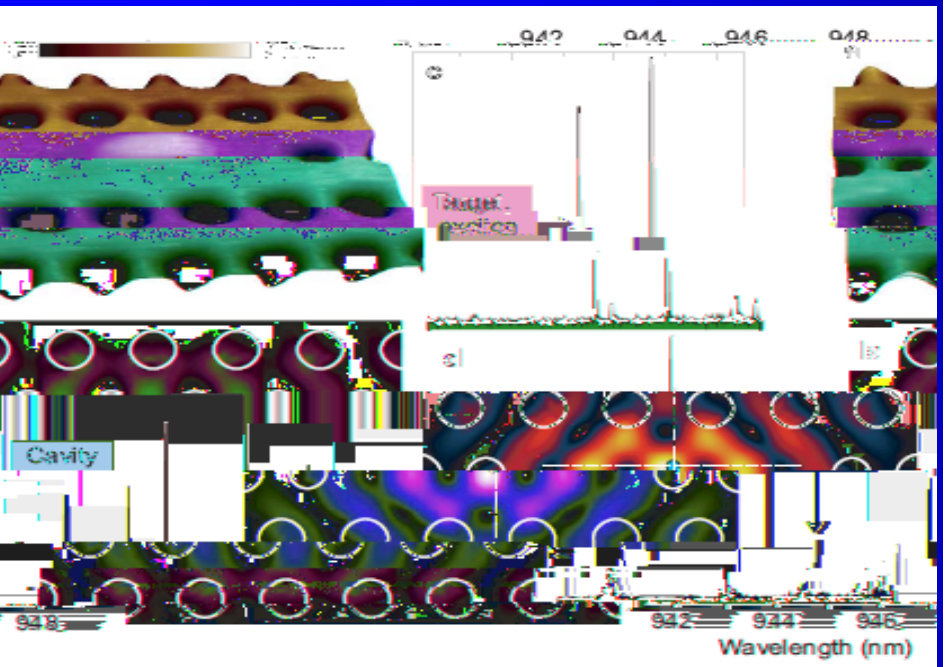

Figure 1 | Positioning a photonic crystal cavity mode relative to a si
a hill of material on the surface arising from a QD buried 63 nm belo
height scale is depicted by the colour bar. **b**, Electric field intensity o
photonic crystal cavity mode showing that the location of the buried
indicated by the teal dot, overlaps the field maximum. The field inte
ranges from zero (black) to a maximum (white), going through blue, r
yellow. **c**, Photoluminescence spectrum before cavity fabrication of a
QD, which was selected for cavity coupling on the basis of clear emis
from a few discrete excitonic transitions. **d**, Photoluminescence spect
from the same QD after cavity fabrication, showing emission fro
at 942.5 nm.

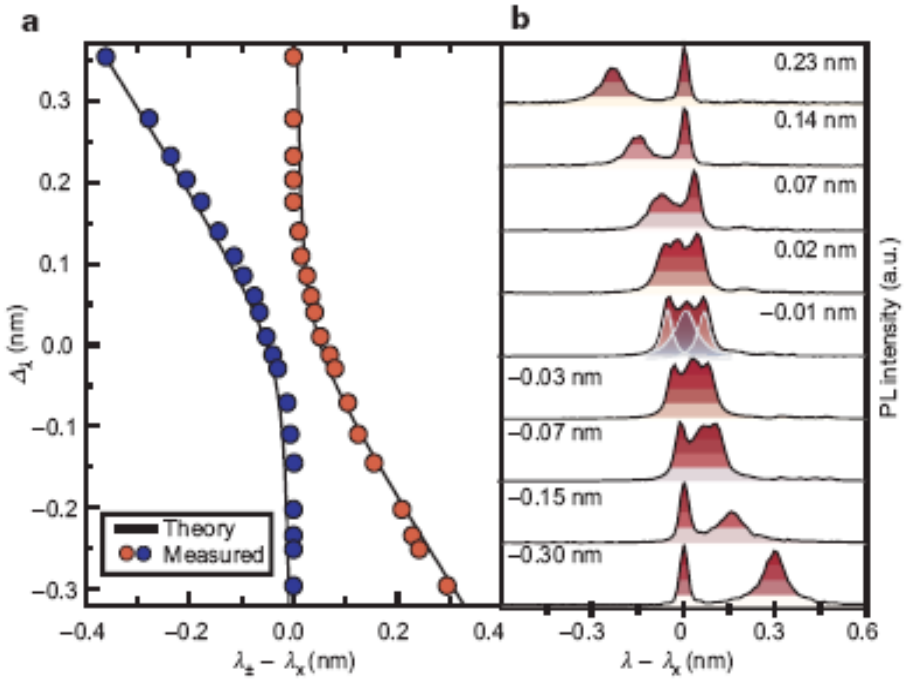

Figure 3 | Characteristics of the strong-coupling regime in the spectral domain. **a**, Wavelength of the polaritons for various detunings, Δ_λ. Calculated spectral peak positions describing the strongly coupled system are plotted as solid lines, with measured peak positions extracted from photoluminescence plotted in red and blue dots. **b**, Spectra of the two anticrossing polariton states near zero detuning. An additional peak is identified as the pure photonic state of the cavity. Values of Δ_λ are shown for each spectrum. PL, photoluminescence; a.u., arbitrary units.

B.

z z z

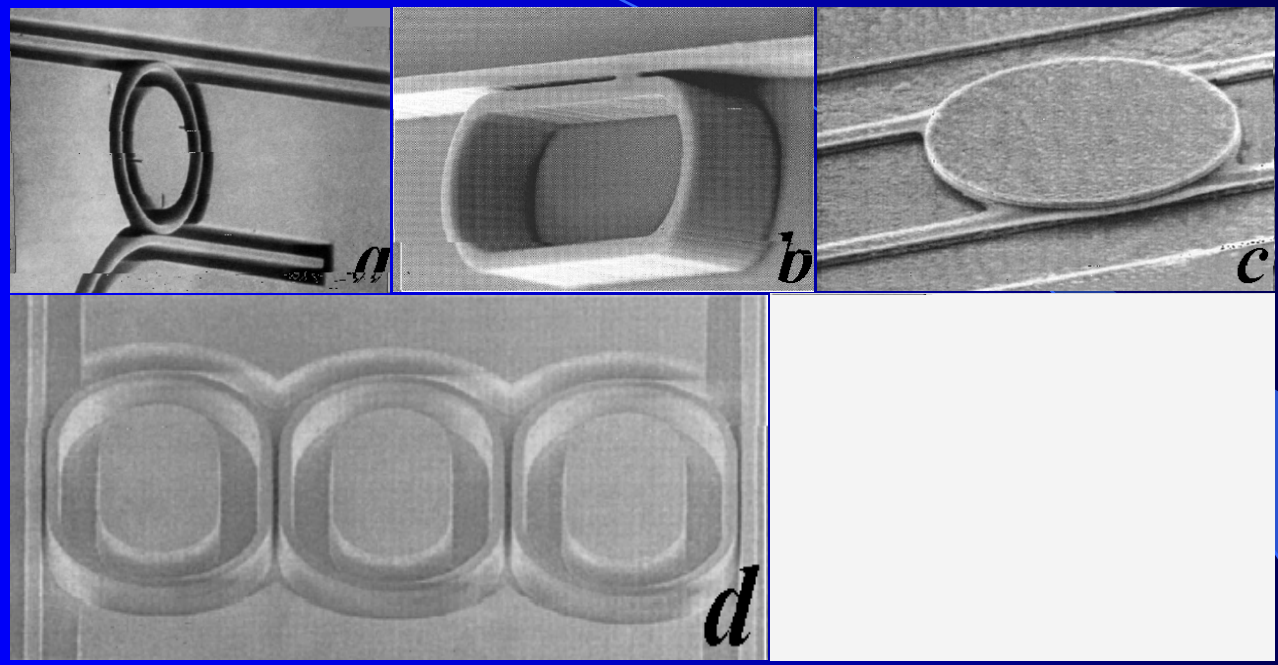
a
b
c
d

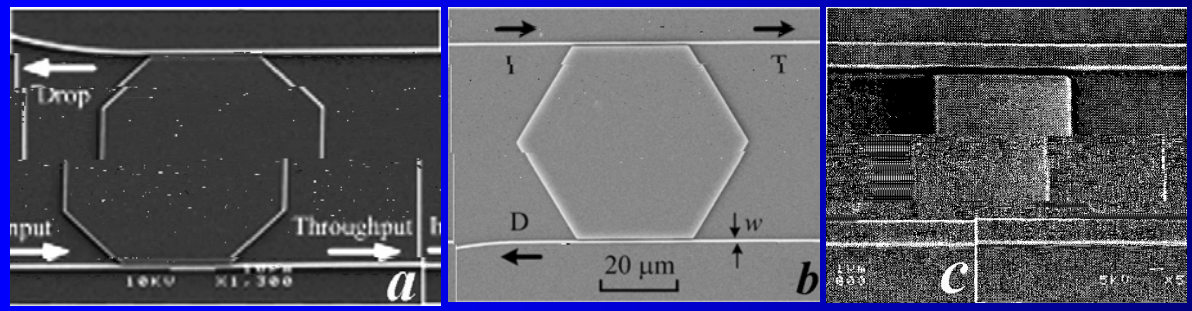
Drop
Throughput
a
T
D
w
20 μm
b
c

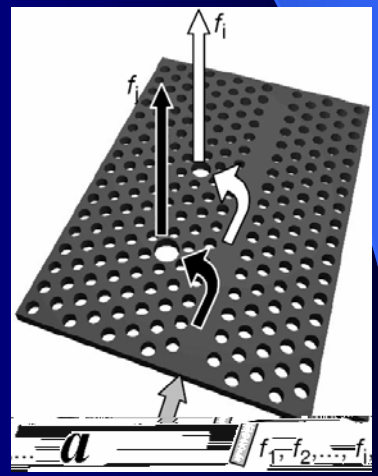
f_i
f_j
a
$f_1, f_2, \ldots, f_i$

微腔光学滤波器：

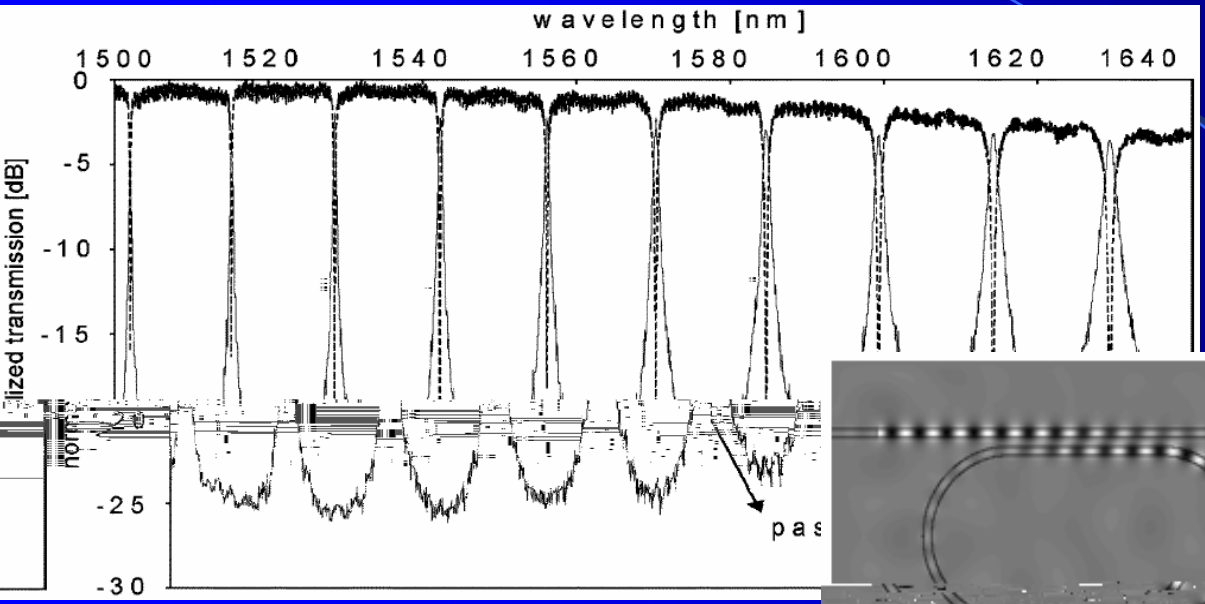
wavelength [nm]
1500
1520
1540
1560
1580
1600
1620
1640
0
-5
-10
-15
-25
-30
ized transmission [dB]
nor
pas

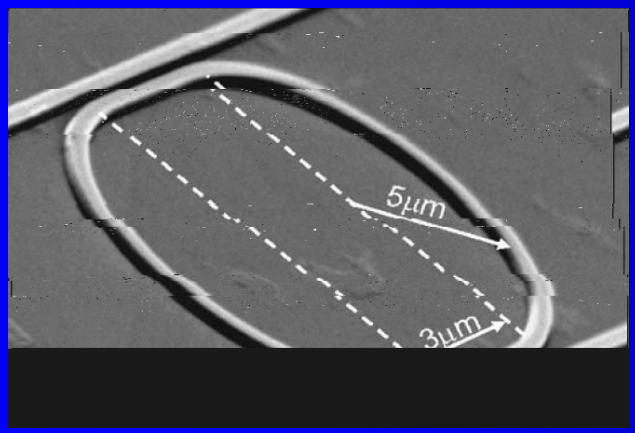
5μm
3μm

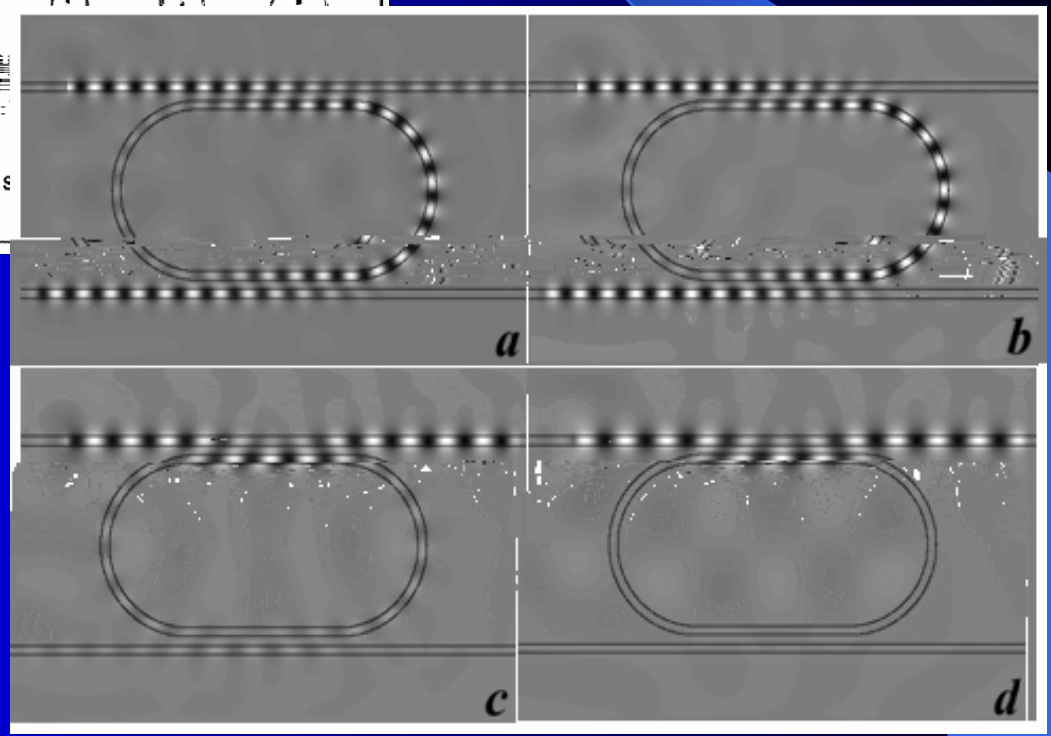
a
b
c
d

Q. Xu, et al, “Micrometre-scale silicon electro-optic modulator,” Nature, vol.435, p.325(2005)

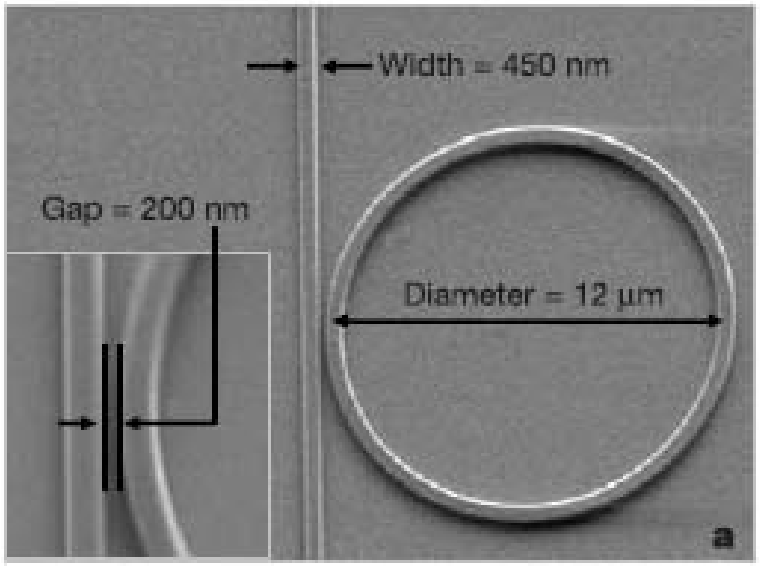

Figure 2 | SEM and microscope images of the fabricated device. **a**, Top-view SEM image of the ring coupled to the waveguide with a close-up view of the coupling region. **b**, Top-view microscope image of the ring resonator after the metal contacts ar[illegible]ed. The metal contact on the central p-doped region of the ring goes over the ring with a 1-μm thick silicon dioxide layer between the metal and the ring.

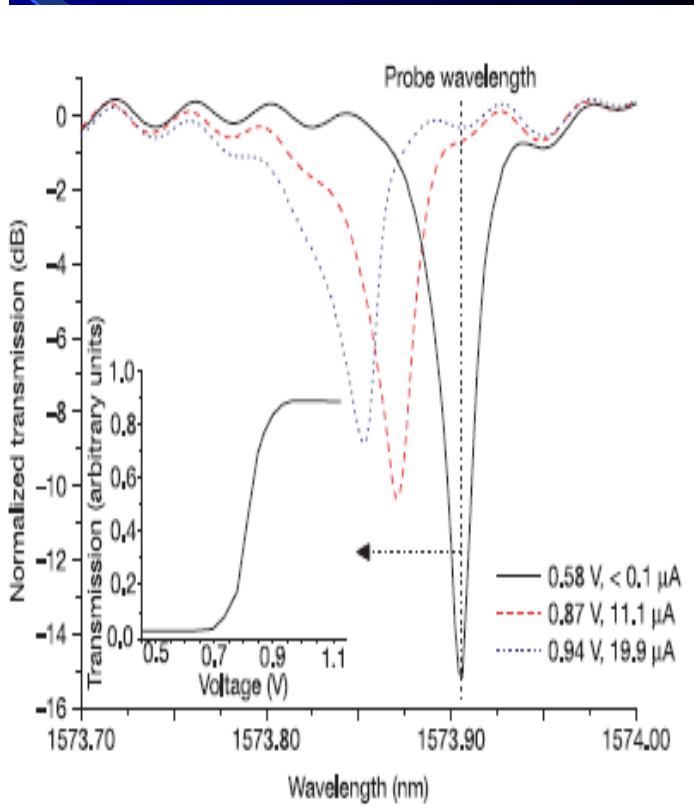

K.Preston, et al, Opt. Exp., vol.15, p.17284(2007)

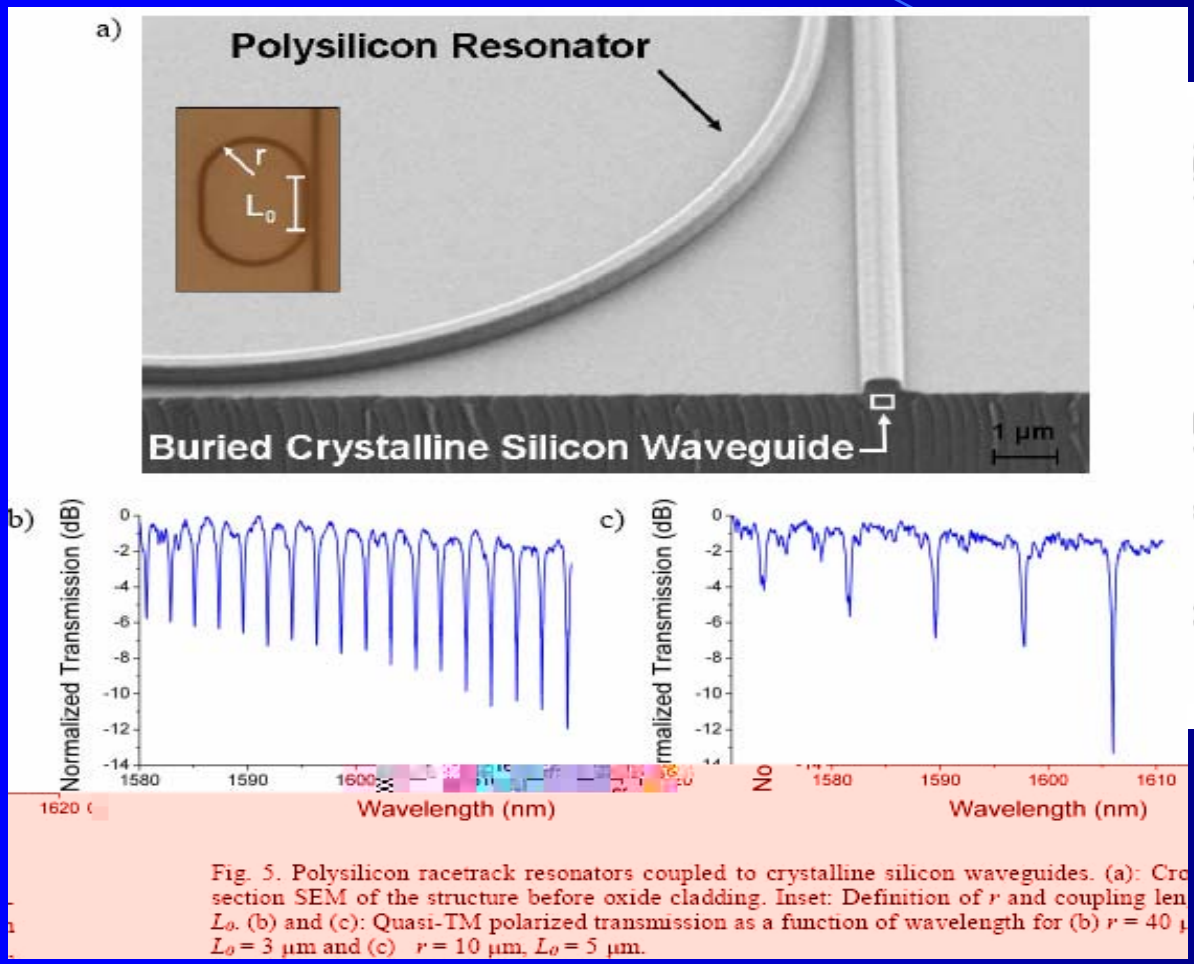

Fig. 5. Polysilicon racetrack resonators coupled to crystalline silicon waveguides. (a): Cro
section SEM of the structure before oxide cladding. Inset: Definition of r and coupling len
L_0. (b) and (c): Quasi-TM polarized transmission as a function of wavelength for (b) $r = 40$ μ
$L_0 = 3$ μm and (c) $r = 10$ μm, $L_0 = 5$ μm.

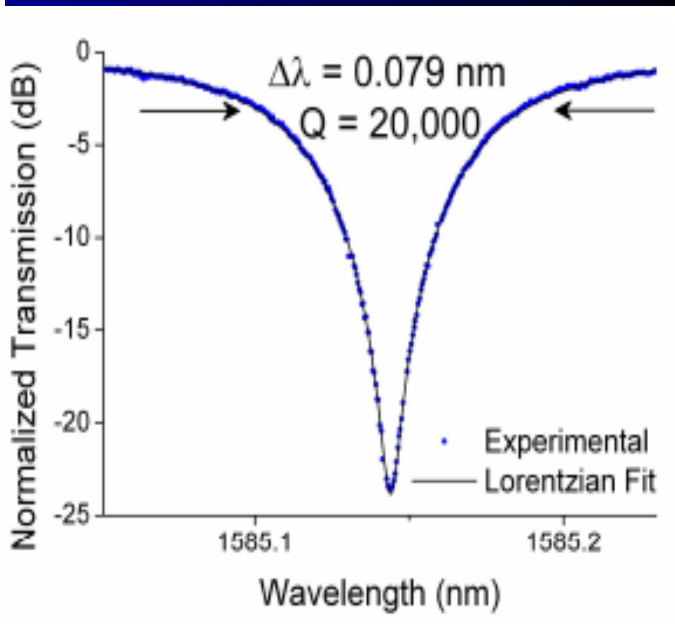

( )

$$g^{(2)}(\tau) = \langle I(t)I(t+\tau)\rangle / \langle I(t)\rangle^2$$

Box 1 Photon-correlation measurements

huang3

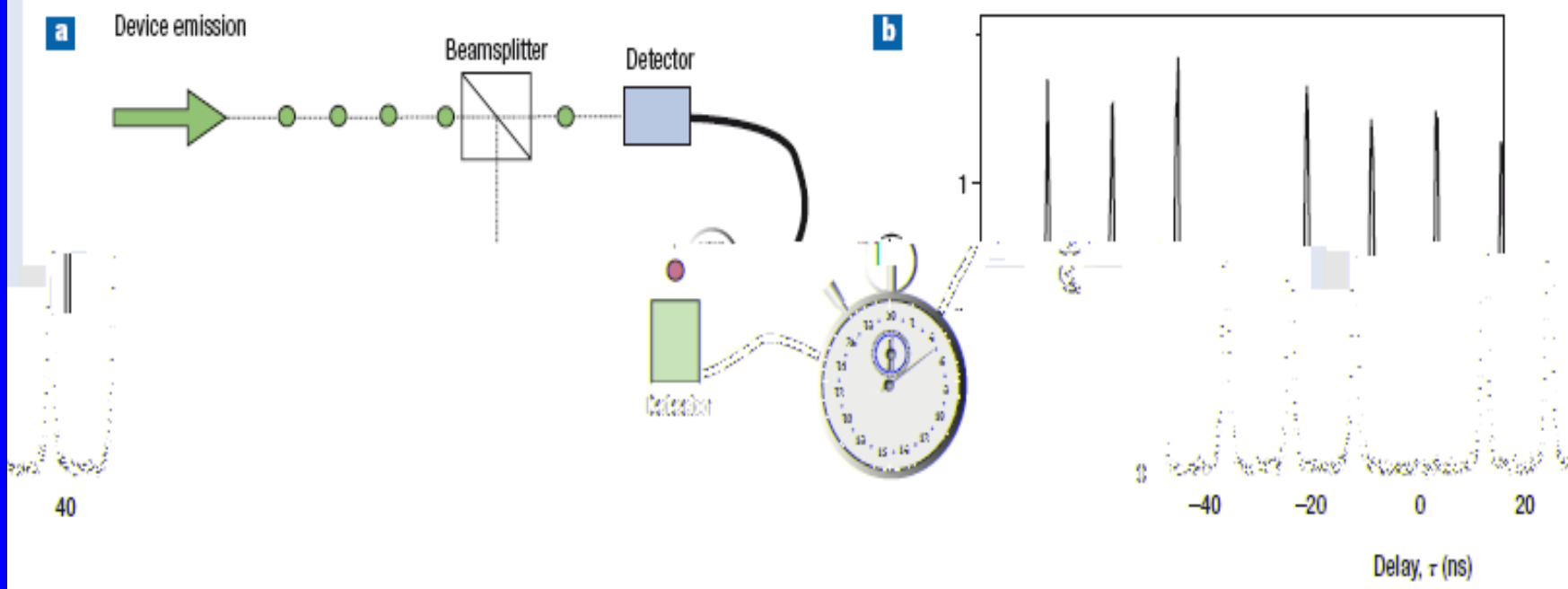

ction of the

Figure B1 Measuring the correlation. **a**, Schematic of the set-up used for photon-correlation measurements. **b**, Second-order correlation fun
exciton emission of a single dot in a pillar microcavity. Reproduced with pemission from ref. 41. Copyright (2005) OSA.

huang3 yzhuang, 2008-3-6

A. J. SHIELDS,"Semiconductor quantum light sources," Nature Photonics, vol.1, p.215(2007)

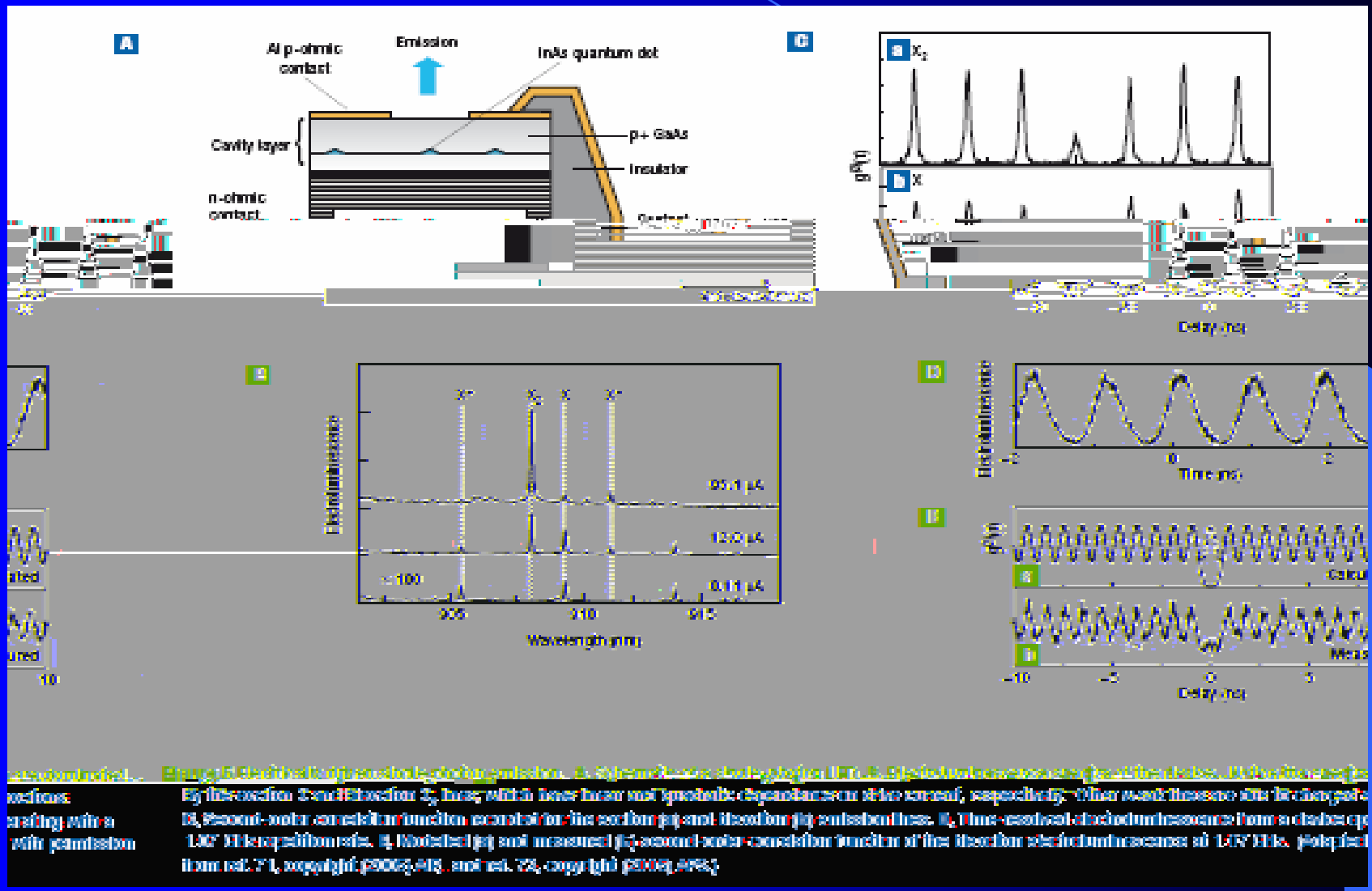

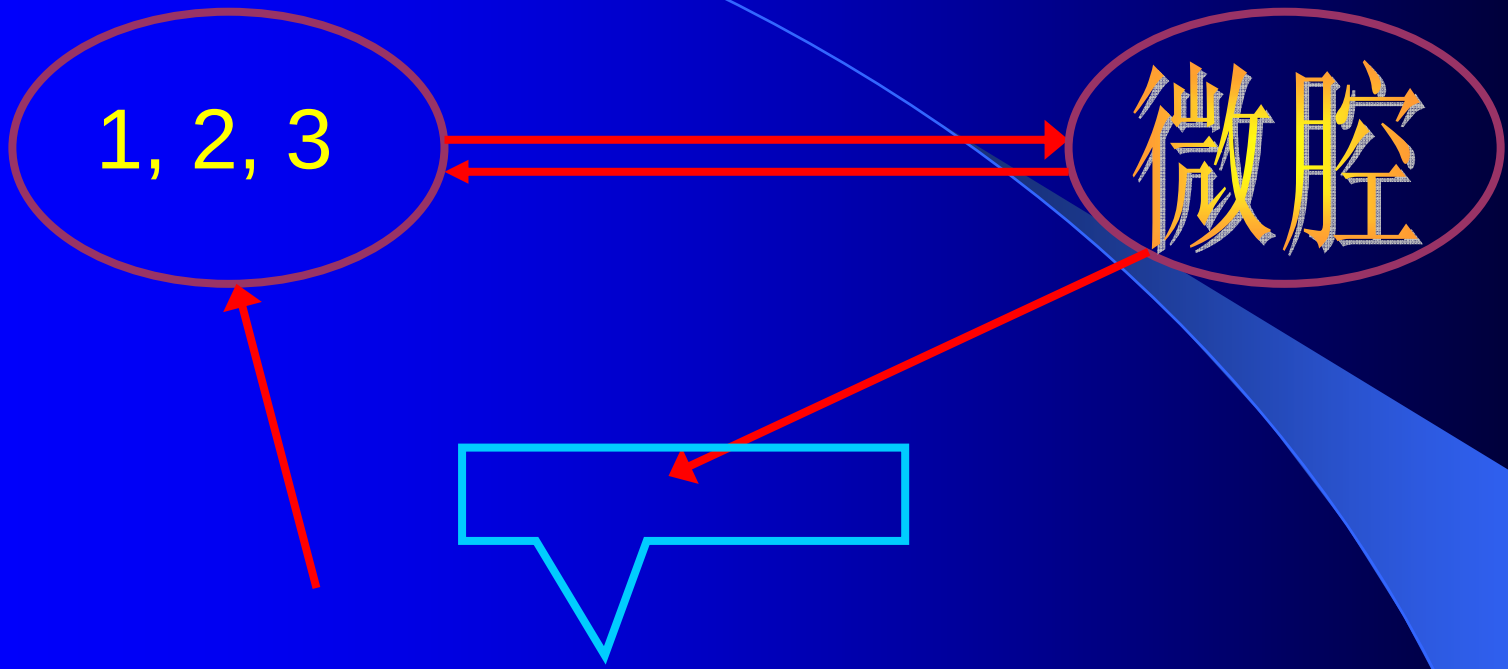
1, 2, 3
微腔

……

Methods for obtaining directional emission

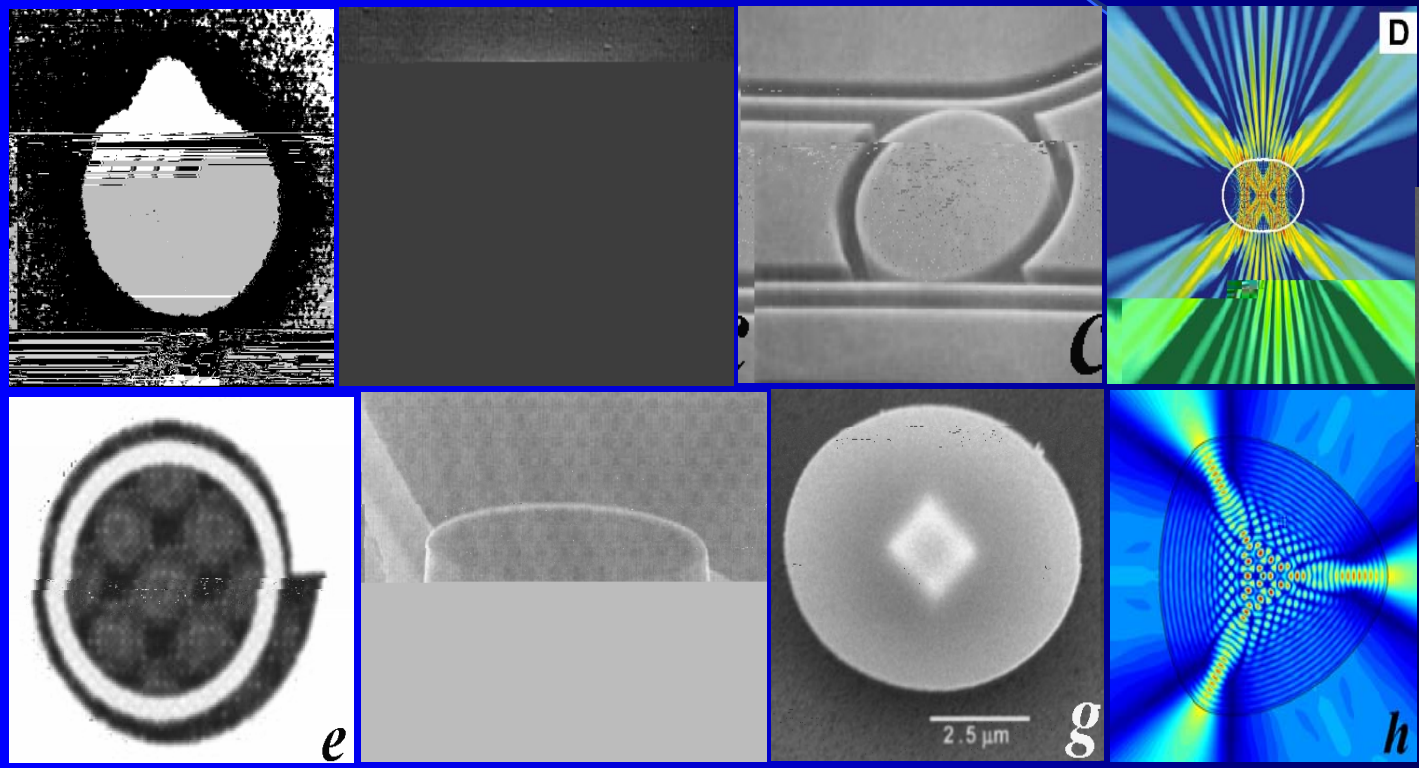

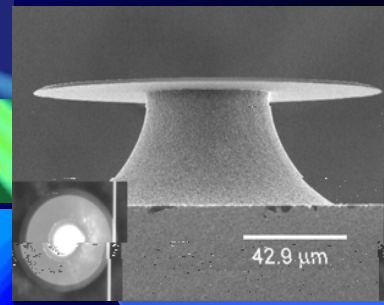

APL,83,797(2003)

Appl.Phys. Lett., (a)62, 561(1993), (b)65,3167(1994), (e)83, 1710(2003),(g)84, 861(2004); (c)J. Lightwave. Technol., 15, 2154(1997); (d) Science, 280, 1556(1998); (f) IEEE Photon. Technol. Lett., 15,1330(2003); (h) Phys. Rev. Lett., 93, 133902(2004)

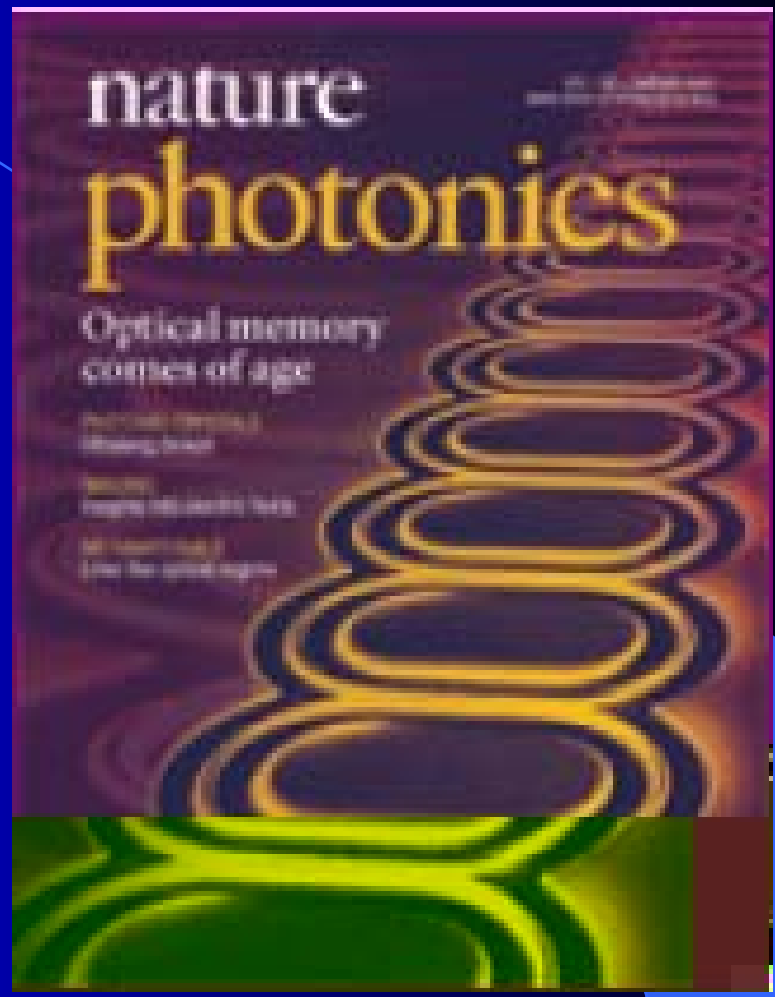

WG

S.-Y.Lee, "**Quasiscarred Resonances in a Spiral-Shaped Microcavity,**" Phys. Rev. Lett., vol.93, 164102(2004)

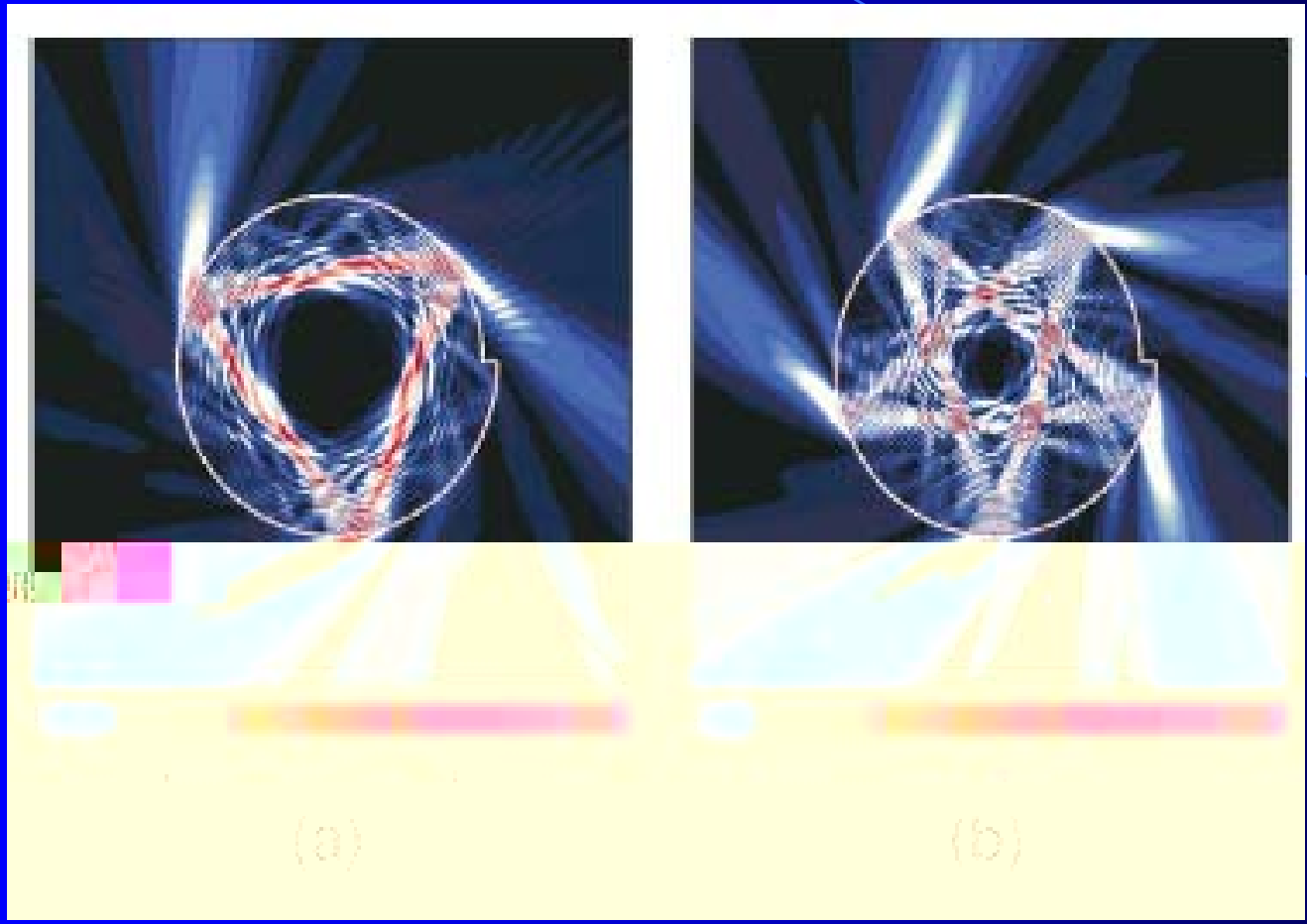

FIG. 3 (color). Field intensity plots of quasiscarred resonances in the spiral-shaped microcavity. (a) *n* = 2 and *nkR* = (109.70, -0.1128). (b) *n*= 3 and *nkR* =(109.59, -0.1127). In figures, the field intensity is normalized by scaling the maximum intensity as one.

huang5 yzhuang, 2008-3-6

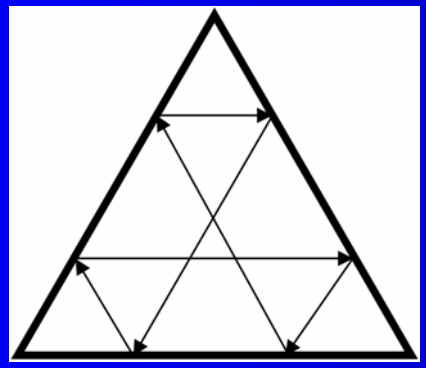

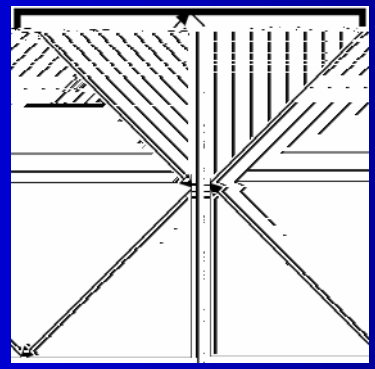

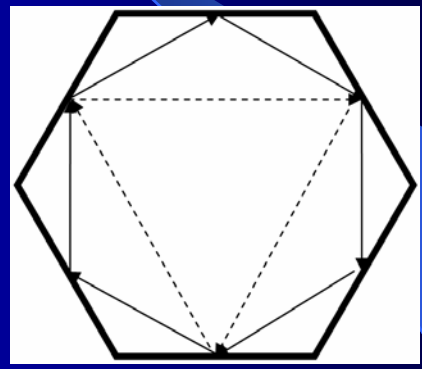

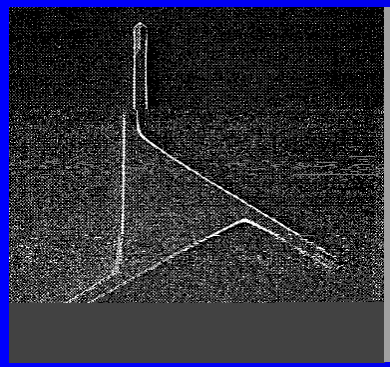

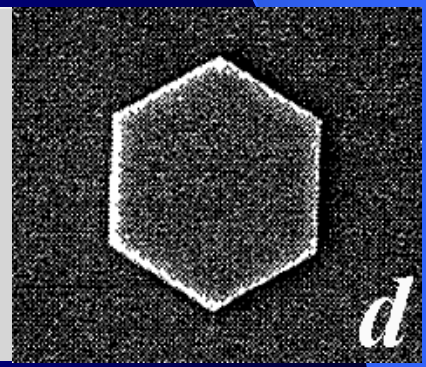
d

II. Equilateral Triangle Resonators (ETR) Lasers

Special type of whispering-gallery cavity

Unfolding mode light ray, ETR is equivalent to a deformed Fabry-Perot cavity

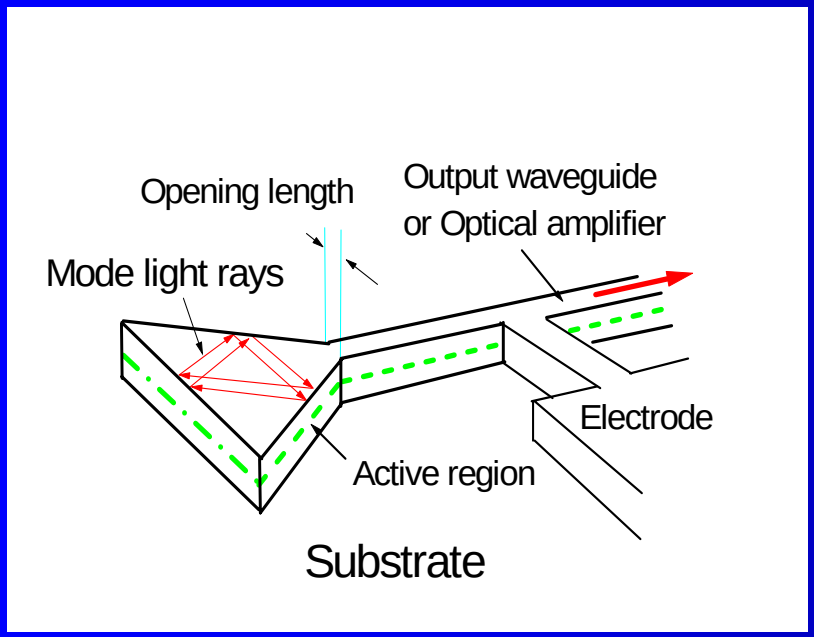

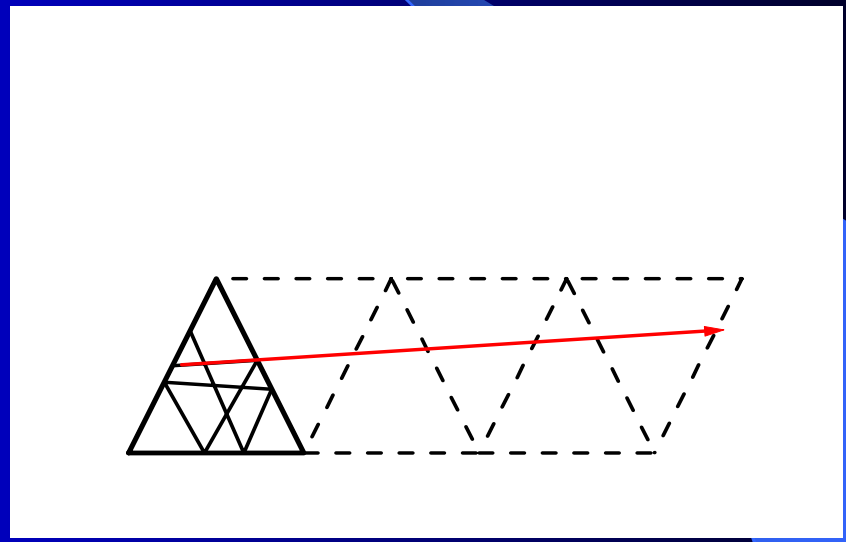

Y.Z. Huang et al, IEEE J. Sel. Topics Quantum. Electron., vol. 12, pp.59-65(2006)

Transverse and longitudinal eigenvalue equation

$$_{m}\quad\frac{\sqrt{3}\,a}{4}\qquad\frac{(m\quad 1)}{2}$$

$$_{l}\quad\frac{3\,a}{2}\qquad 3\qquad 2\,l$$

$$2\tan\quad^{1}\left(\frac{\sqrt{3}\quad l}{2\quad 1}\right)\qquad\frac{1\quad(\quad 1)^{m}}{2}$$

***l* and *m* are longitudinal and transverse mode numbers, and mode wavelength is:**

$$_{m,l}\qquad\frac{3Na}{\sqrt{(2l\quad 3\quad /\quad)^{2}\qquad 3(m\quad 1)^{2}}}$$

Mode field intensity for an ETR lasers with output waveguide obtained by FDTD simulation

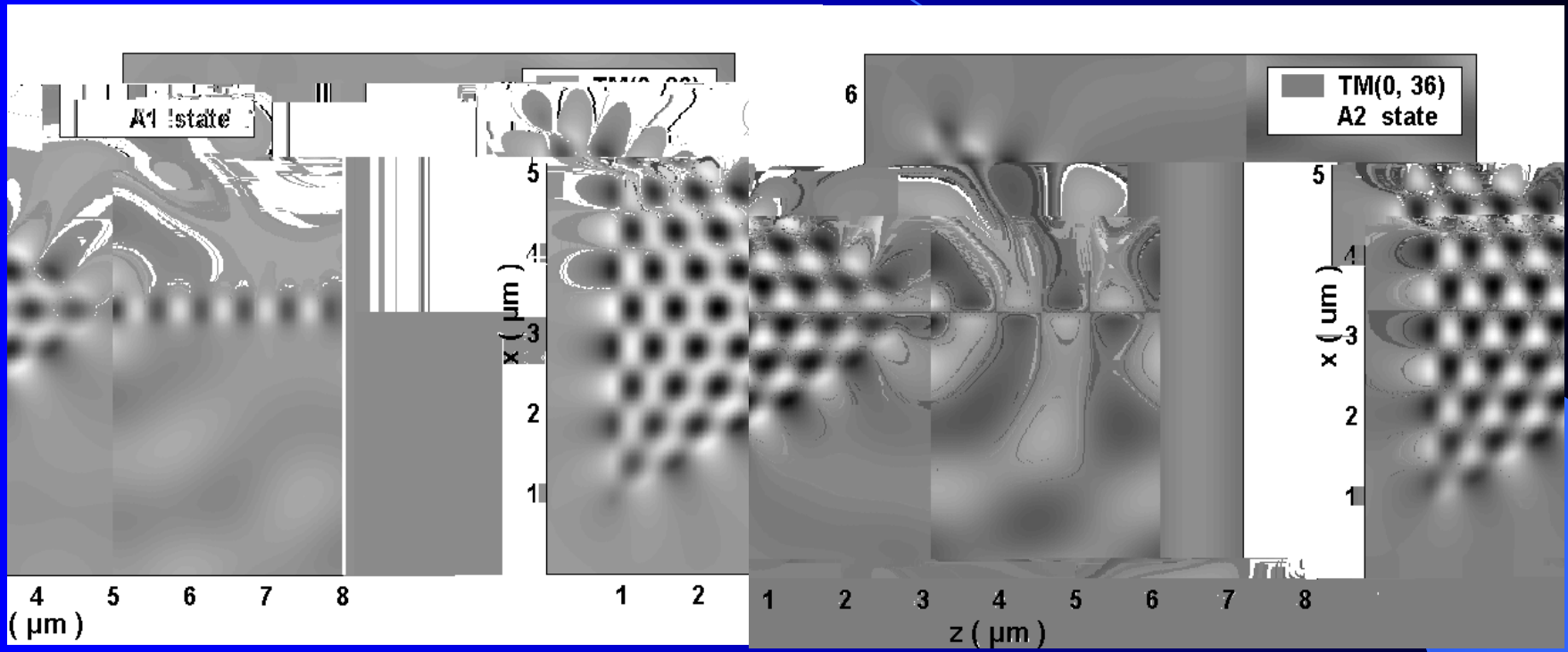

The side-length and inner refractive index of ETR is 5 μ m and 3.2 respectively. The width of output waveguide is 0.3 μ m. The field intensity in the region of z >5 μ m is magnified 5 times.

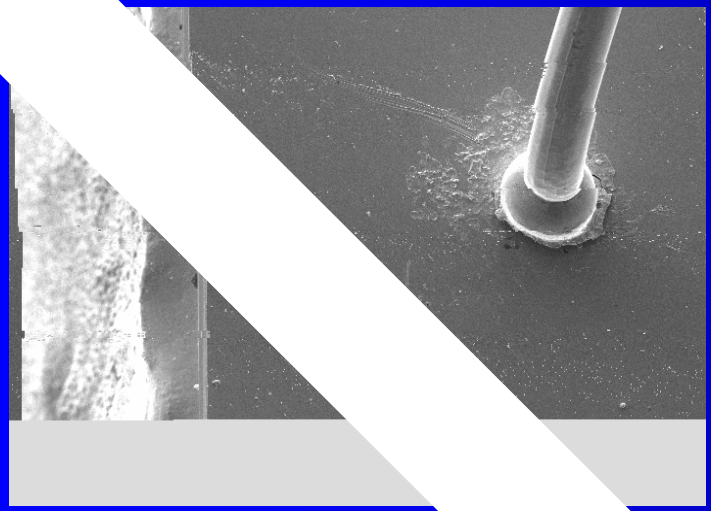

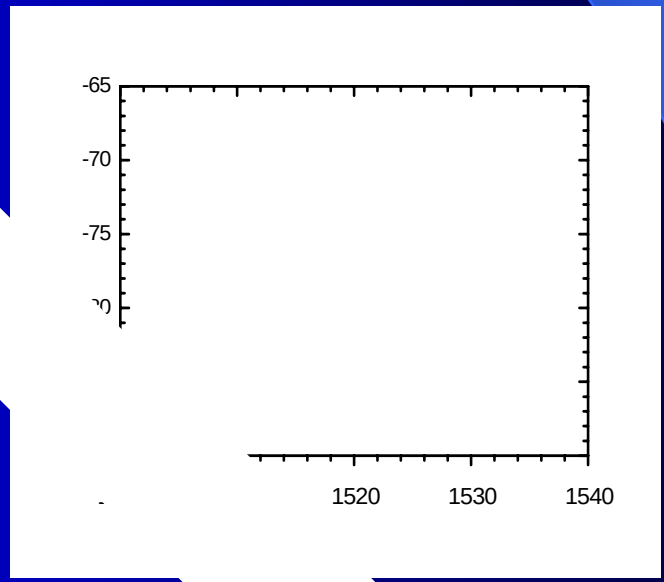
-65
-70
-75
1520
1530
1540

10 m -
, 295K .

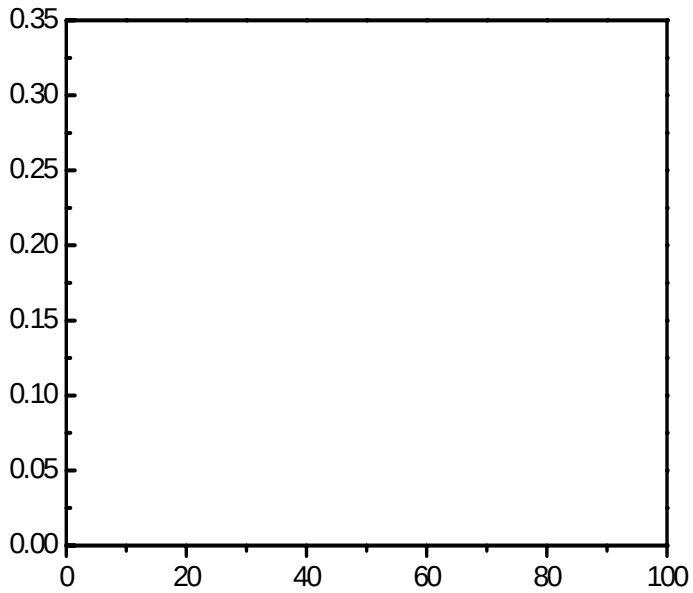

III. Mode Confined in Rectangular Microresonator

1. Modes confined in square resonator with mode indices (*p*,*q*) denoting the numbers of wave nodes in the *x* and *y* directions

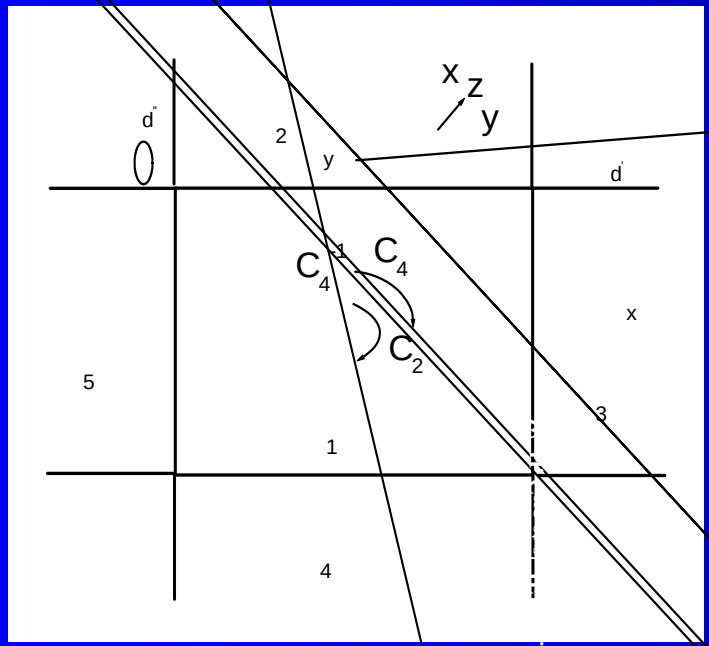

Mode field distribution and eigenvalue equations:

$$F_{zx}^{p}\quad \begin{cases} \cos(\ {}_{x}x\quad {}_{x}) & |x|\quad a/2 \\ \cos(\ {}_{x}a/2\quad {}_{x})\exp[\quad {}_{x}(x\quad a/2)] & x\quad a/2 \\ \cos(\quad {}_{x}a/2\quad {}_{x})\exp[\ {}_{x}(x\quad a/2)] & x\quad\ a/2 \end{cases}$$

$$F_{zy}^{q}\quad \begin{cases} \cos(\ {}_{y}y\quad {}_{y}) & |y|\quad b/2 \\ \cos(\ {}_{y}b/2\quad {}_{y})\exp[\quad {}_{y}(y\quad b/2)] & y\quad b/2 \\ \cos(\quad {}_{y}b/2\quad {}_{y})\exp[\ {}_{y}(y\quad b/2)] & y\quad\ b/2 \end{cases}$$

$$\begin{matrix} {}^{2} & {}^{2} \\ x & y \end{matrix}\qquad n_1^2 k_0^2$$

$$\begin{matrix} {}^{2} & {}^{2} \end{matrix}\qquad (n_1^2\quad 1)k_0^2$$

$$\begin{matrix} {}_{x}\tan(\ {}_{x}a/2\quad {}_{x}) & x \\ {}_{y}\tan(\ {}_{y}b/2\quad {}_{y}) & y \end{matrix}$$

$= n_1^2/n_2^2$ for TE mode
$= 1$ for TM mode, $v = x, y$

The total internal reflection limits the difference between k_x and k_y, $\quad {}_{v} = 0$ or $\quad /2$ as the corresponding p or q is even or odd number, respectively.

Mode intensity spectrum obtained by FDTD simulation and Pade approximation for a square resonator with sidelength of 2 m and *n*=3.2

TE0,14 **TE0,16**

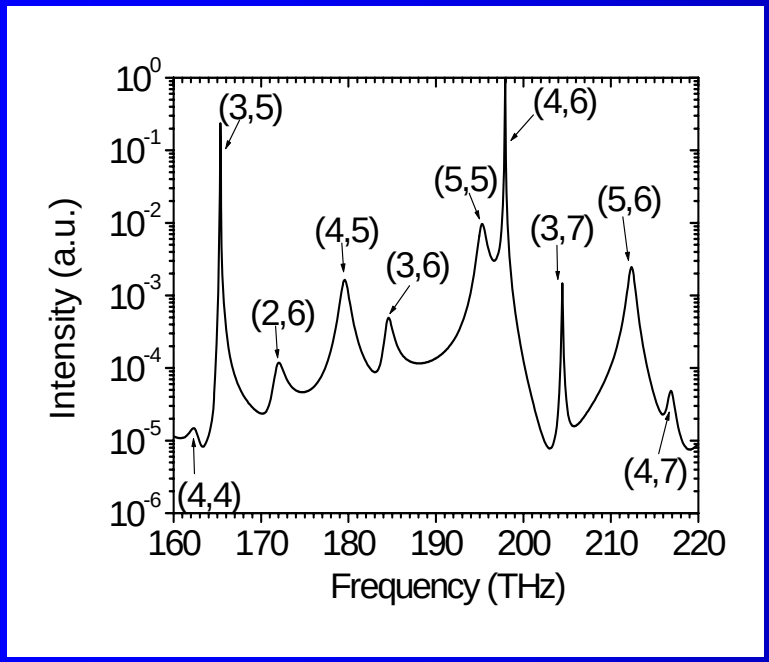

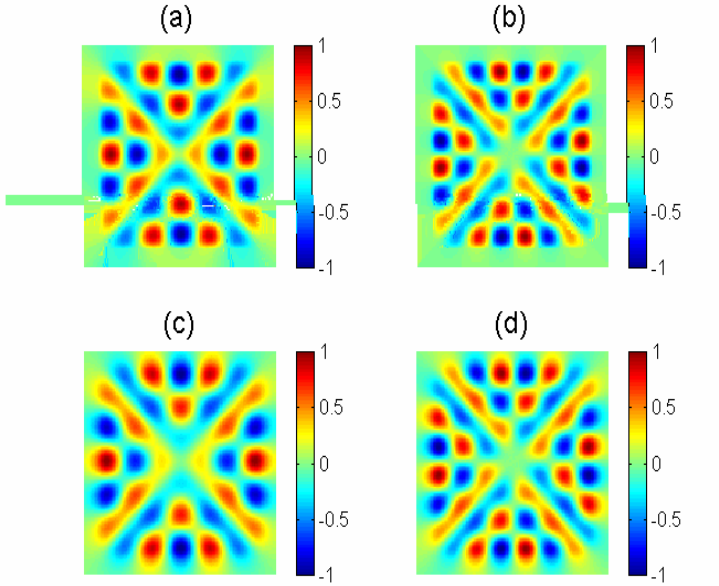

FDTD

Analytical

Mode with same symmetry in x and y directions have high Q-factor.

Mode field patternin a square resonator with a = 2 m and n=3.2.

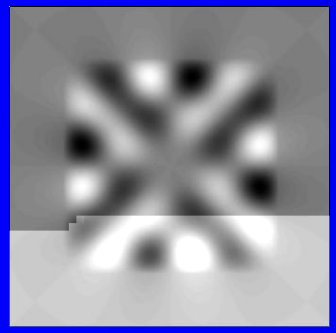

$TE^o(3,5)$

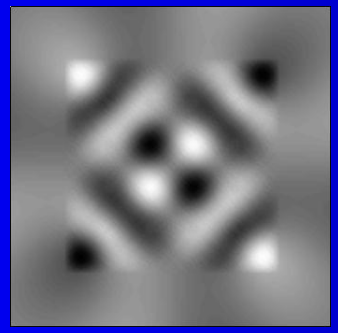

$TE^e(3,5)$

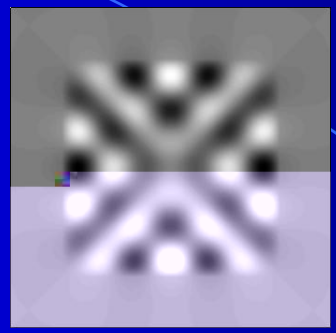

$TE^o(4,6)$

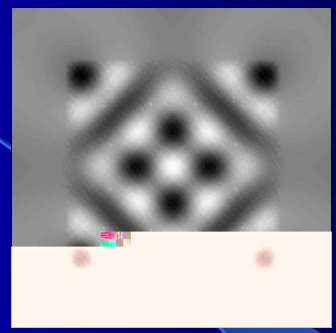

$TE^e(4,6)$

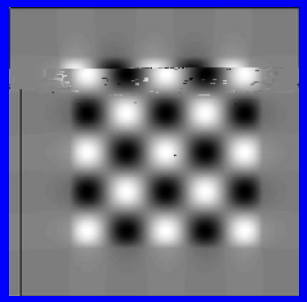

TE(4,4)

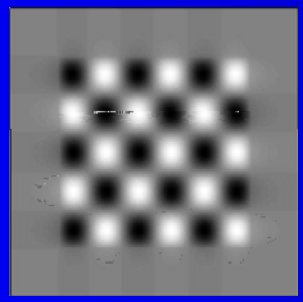

TE(4,5)

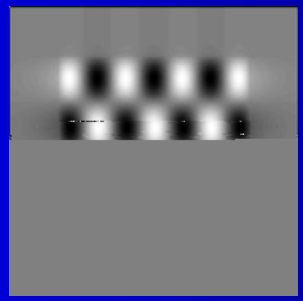

TE(3,6)

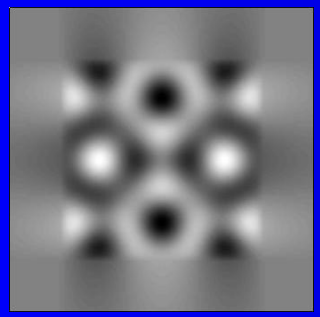

$TE^o(2,6)$

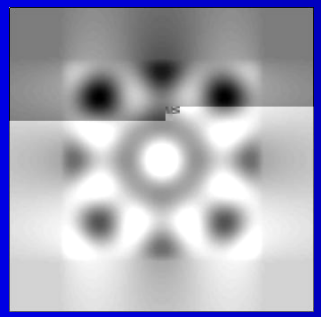

$TE^e(2,6)$

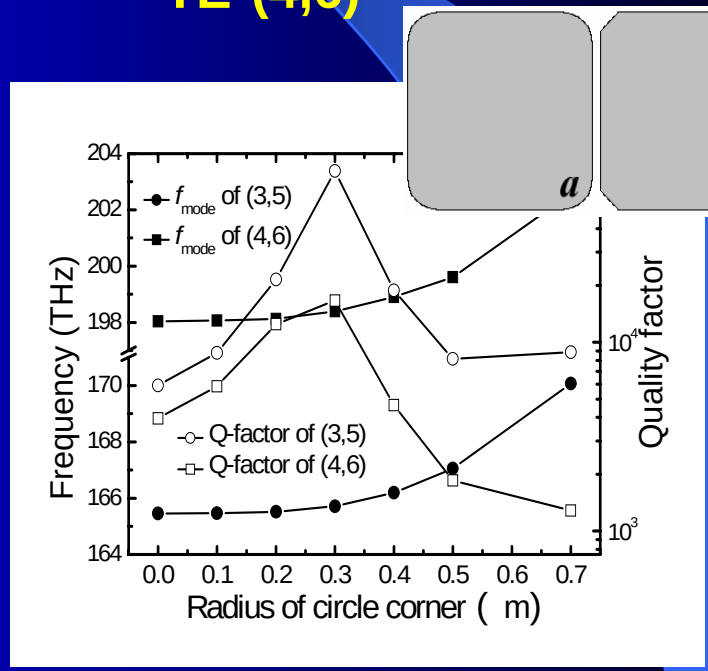

Mode Q-factors even increase in a square with circular corners.

Square resonator fabricated by selected chemical etching technique.

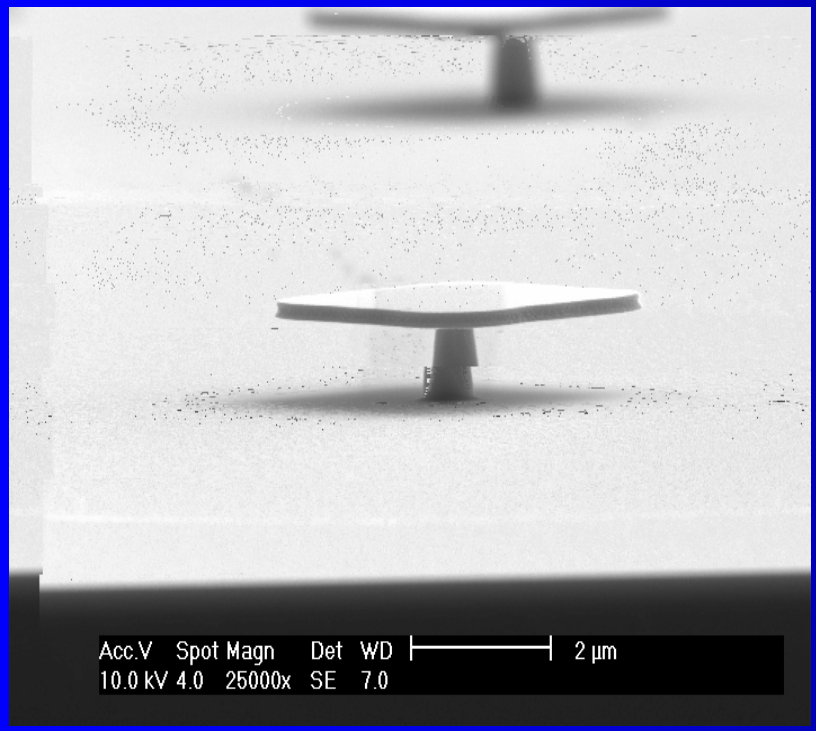

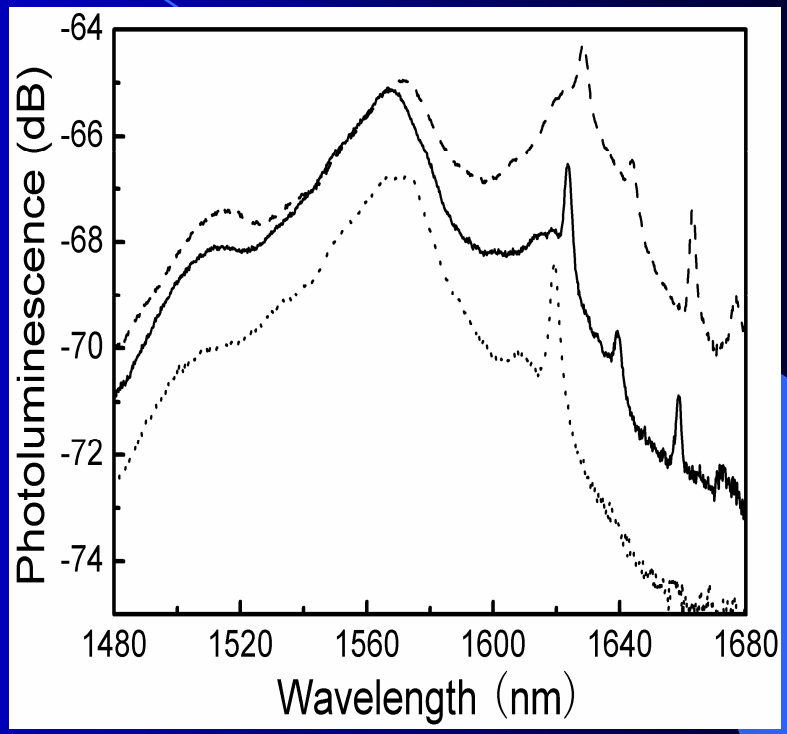

SEM picture and photoluminescence of a square with side length of 7 m.

Y. Z. Huang et al, IEEE Photon. Technol. Lett., vol. 17, p.2589(2005)

Directional emission for square microlasers

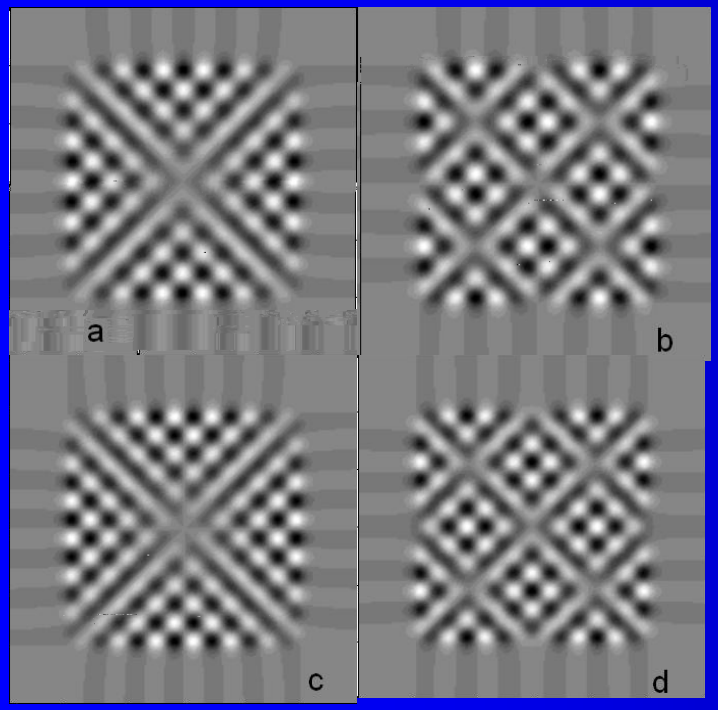

Field distribution of (a)$TM_{10,12}$, (b)$TM_{9,13}$, (c) $TM_{11,13}$, (d) $TM_{9,13}$ in a square with sidelength of 4 m and refractive index 3.2.

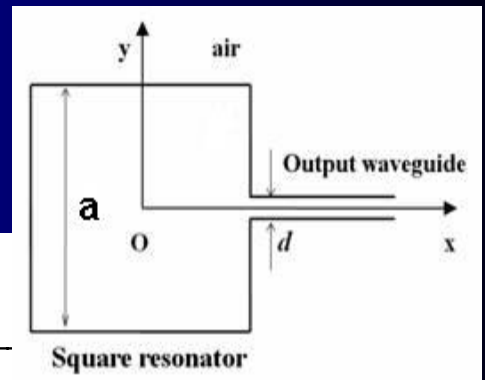

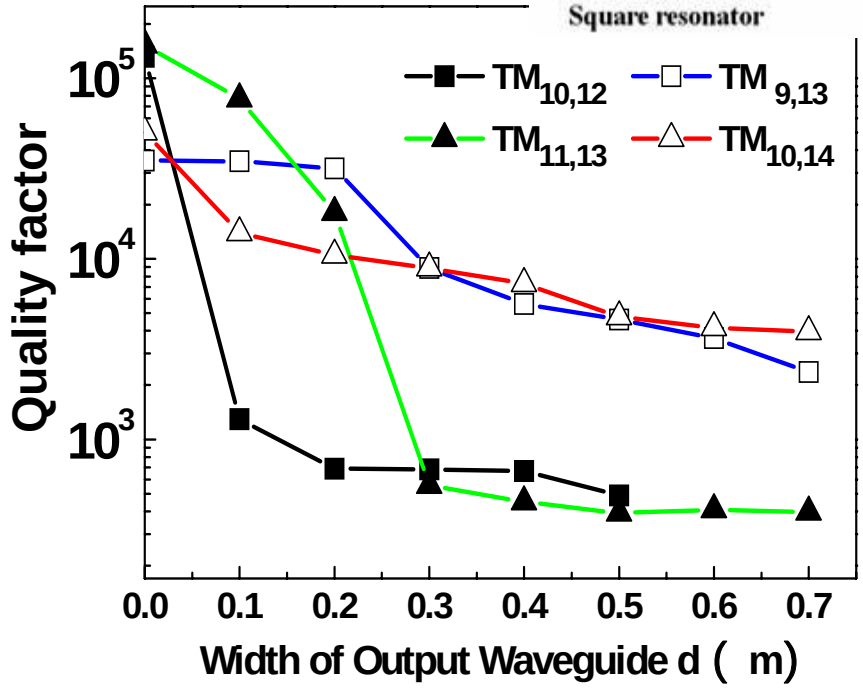

Mode Q-factor versus width of output waveguide

Directional Emission square InGaAsP laser with 20 m side.

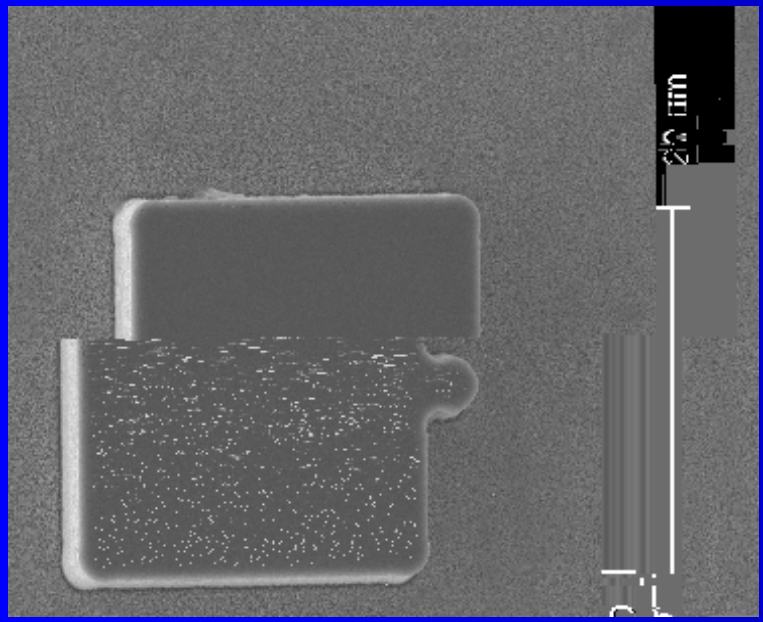

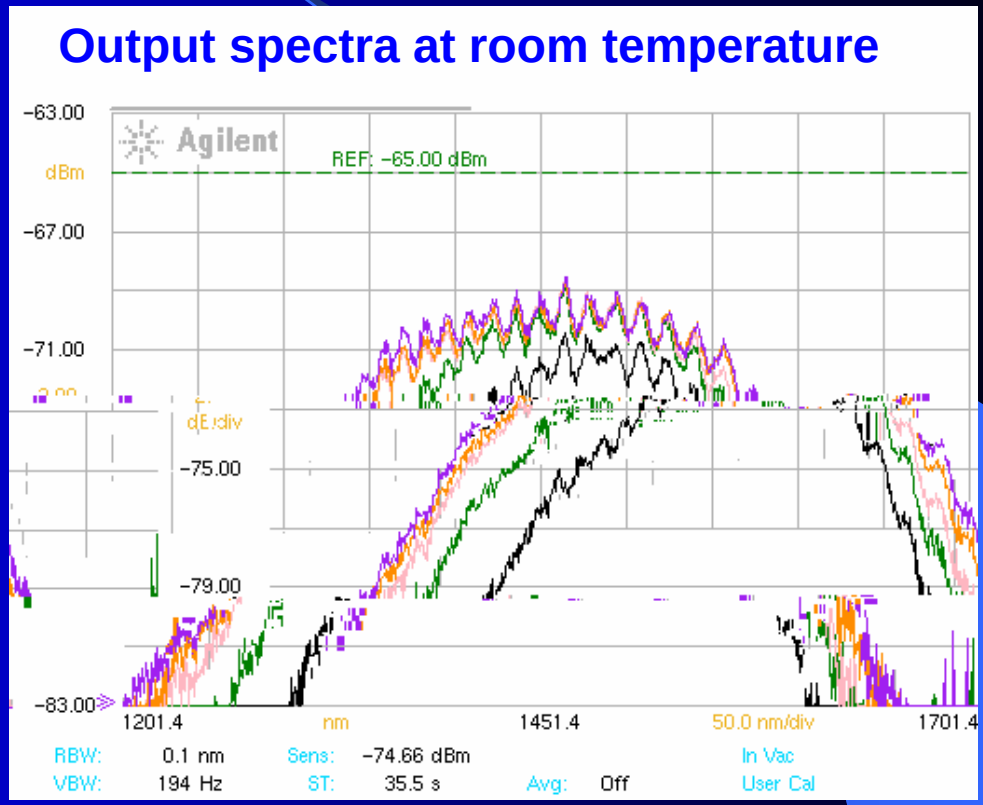

First run. CW electrically operation is realized at 200K.

Derivative resistor is one order larger than the ETR laser. (70~80Ω)

Laser spectrum and output power-injection current curve of a InGaAsP/InP square laser with side length 20 m at 200K.

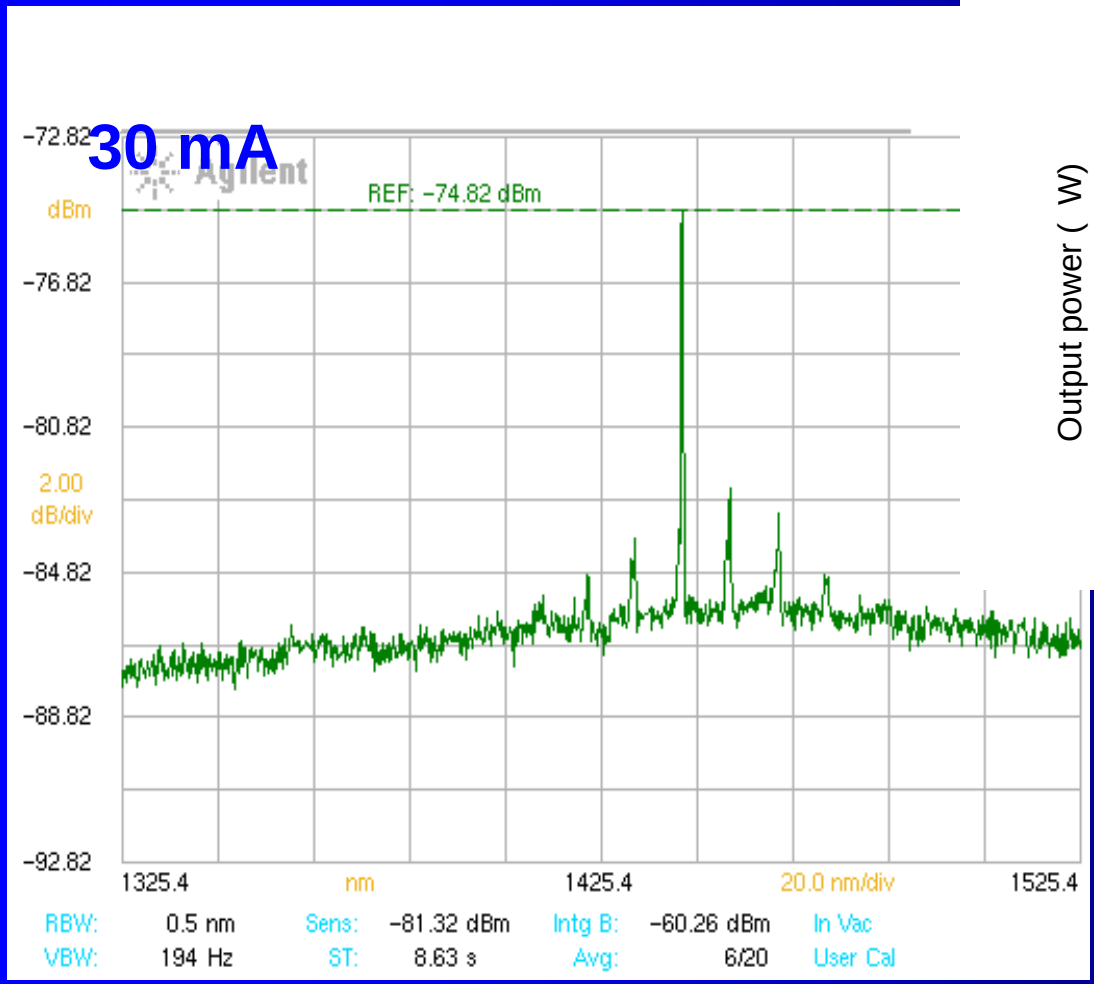

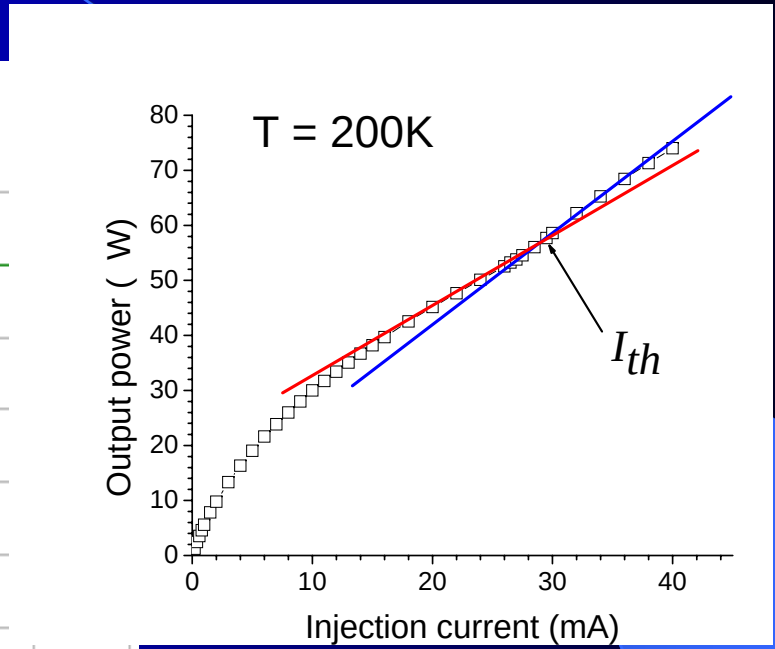

四. 纵向弱波导三维微腔中的高Q值TM模

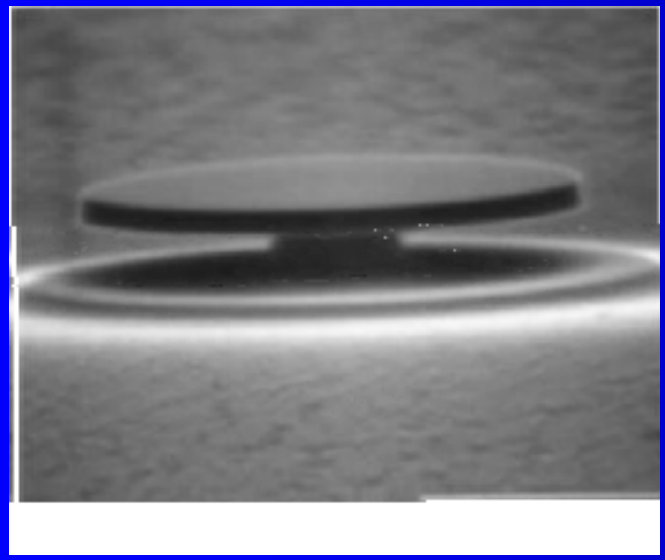

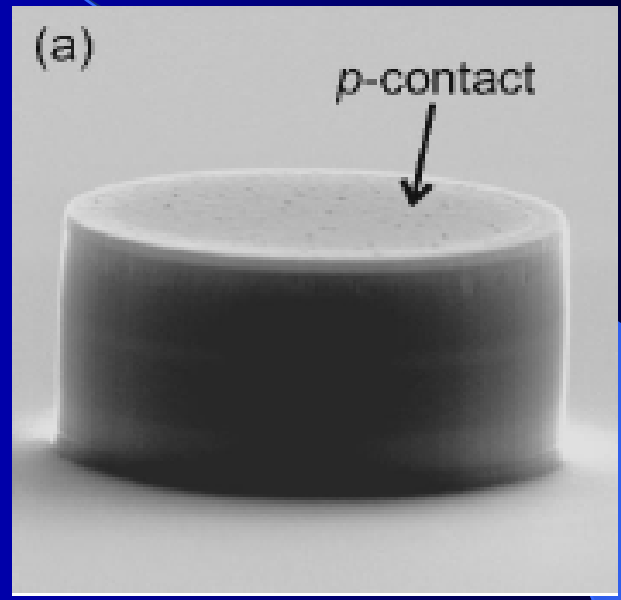

Q ?

Whispering-Gallery Modes (WGMs) in 3D microcylinder

TE and TM modes in 3D microcylinder How to get High-Q modes in microcylinders ?

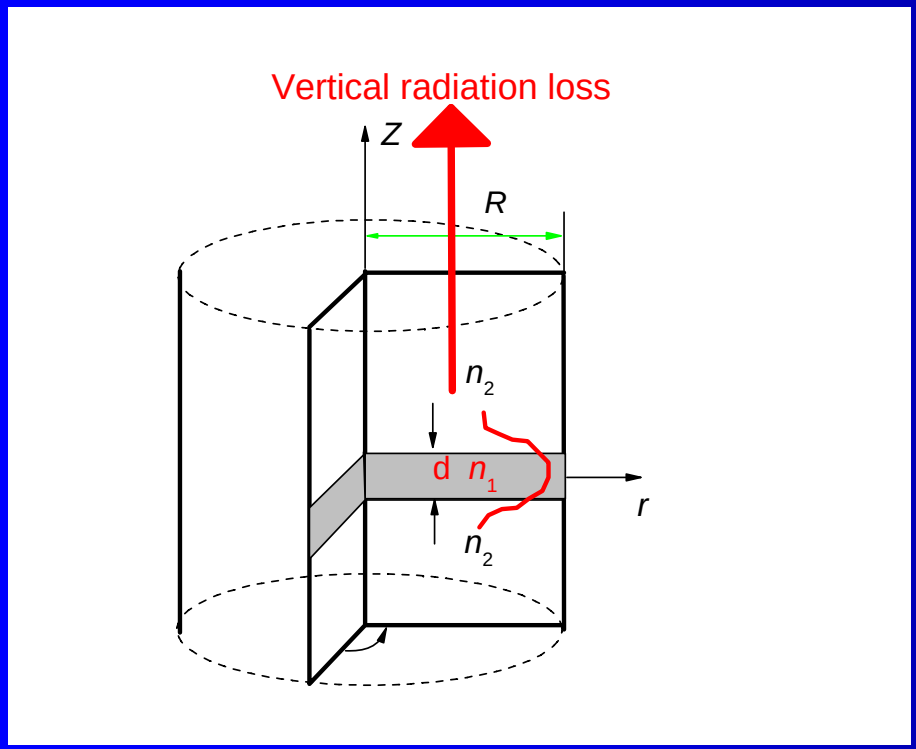

3D finite difference time-domain (FDTD) simulation under circular symmetry 2D case

parameters R = 1 m, d = 0.2 m, n_1 = 3.4.

TE (TM) modes: magnetic (electric) field H_z (E_z) is symmetry to r-Φ plane.

Mode Q-factor versus the refractive index of cladding layer n_2

Mode wavelengths and *Q*-factors for $TE_{7,1}$ and $TM_{7,1}$ WGMs versus n_2. TM mode can have high Q-factor even vertical refractive indices are 3.4/3.2

1 m

*n*2/*n*1=3.4, *d*=0.2 m /*n*2

TE TM Q *n*2 TM

TM Q

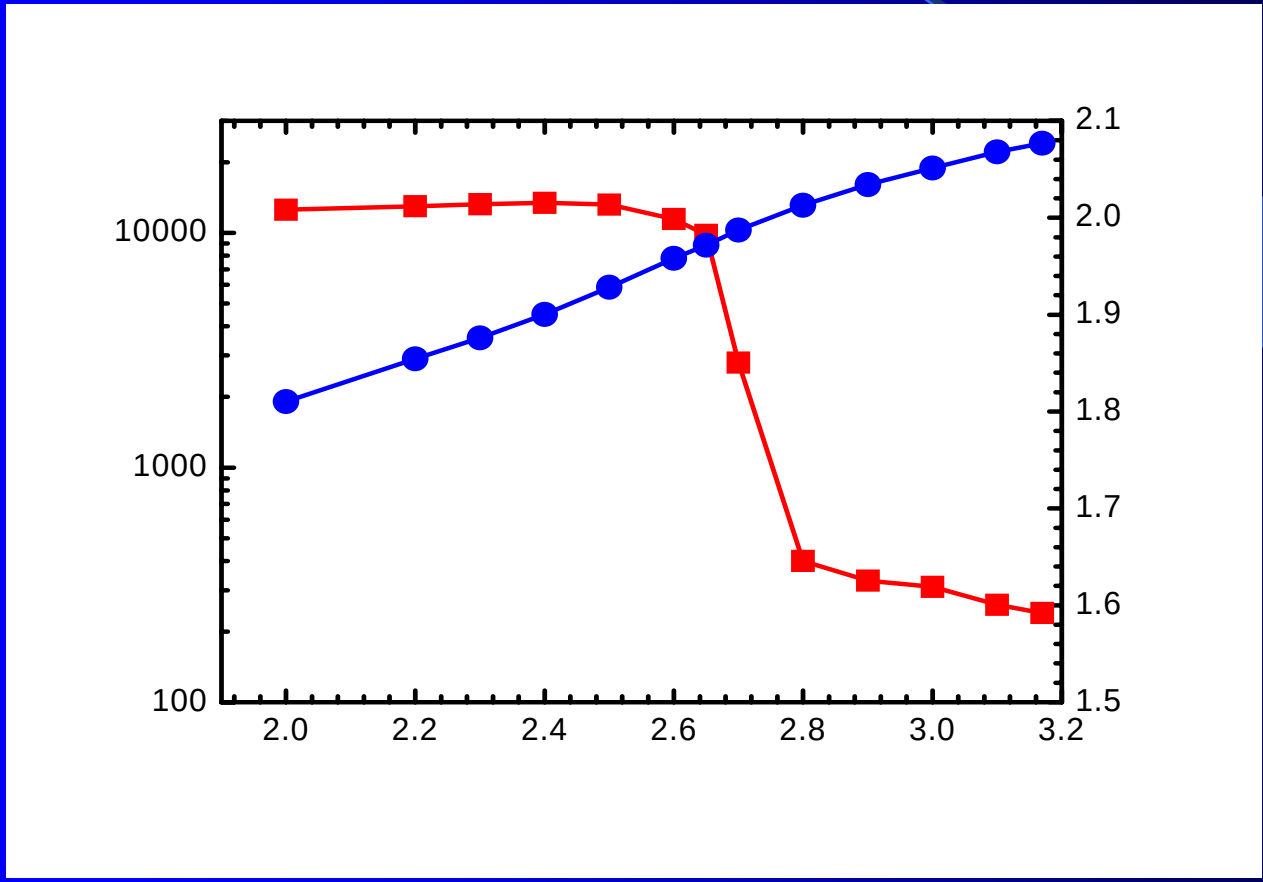

Mode wavelengths of the WGMs under effective index approximation and cut-off wavelength of the same order radiation modes in the cladding layers obtained by the following eigenvalue equation:

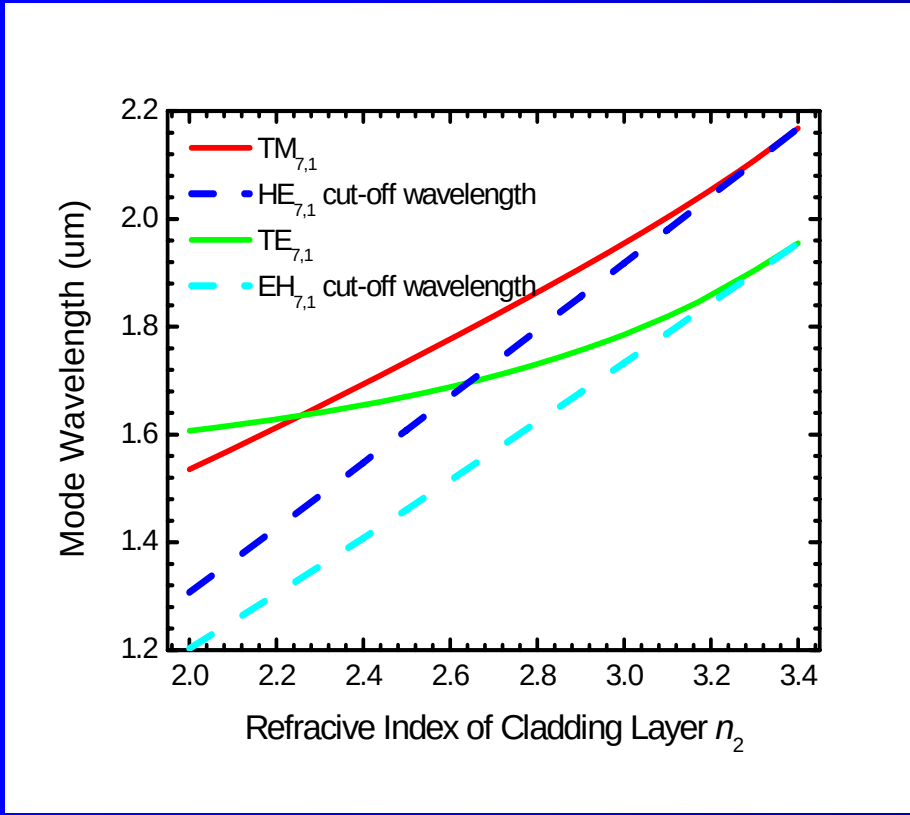

$$J_v(knR)H_v^{(2)}{}'(kR) = \eta\, J_v'(knR)\, H_v^{(2)}(kR)$$

(M. Hentschel et al, Phys. Rev. E66, 056207 (2002))

$n=n_{eff}$ for TE and TM WGMs

$n=n2$ for HE_{off} and EH_{off} radiation modes

$\eta = n$ for TM and HE*off* modes

$\eta = 1/n$ for TE and EH*off* modes

(*R* = 1

m, *d* = 0.2 m, *n*2/ 3.4/*n*2)

When n_2>2.65, $\lambda_{WGM}(TE_{7,1}) < \lambda_{radiation}(HE_{7,1})_{off}$ vertical radiation loss

Mode wavelengths and Q-factors of TE and TM WGMs versus azimuthal mode number obtained by FDTD simulation for the microcyliner with vertical refractive indices 3.4/3.17.

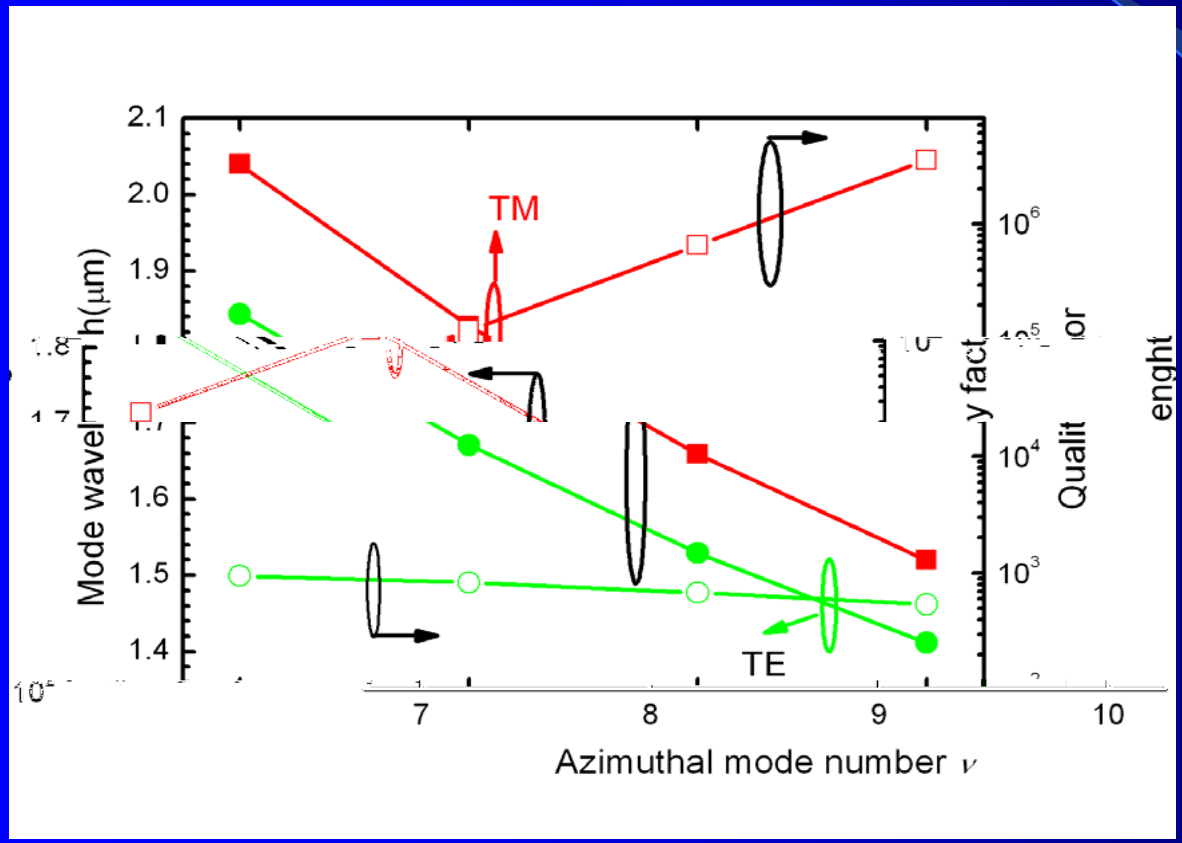

TE WGMs:
$Q \sim 10^2$

TM WGMs:
$Q \sim 10^4 \quad 10^6$

FDTD **TE** **TM** ***Q*** ***ν***

Vertical field distribution of $TE_{7,1}$ WGM at $n_1 = 3.4$ and $n_2 = 2$, 2.5, and 3.17 obtained by FDTD simulation.

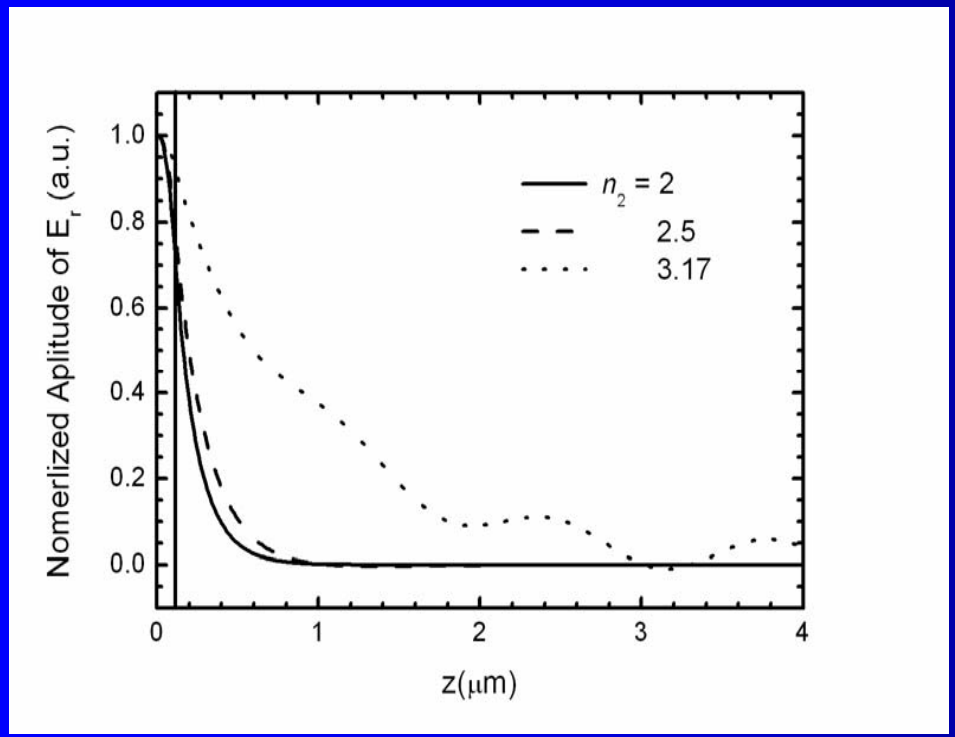

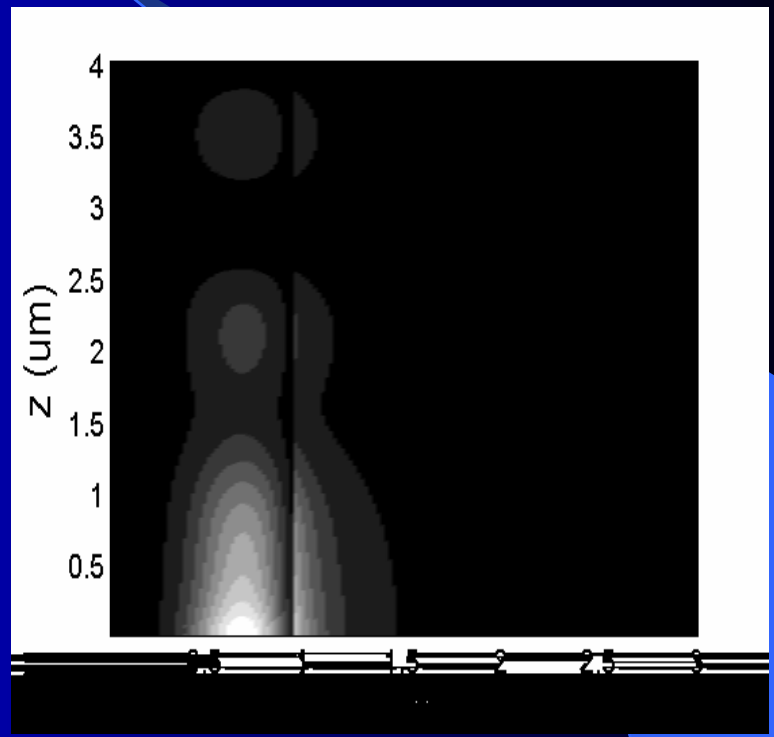

$r = 0.84R$

$n_2 = 3.17$

Vertical field distribution of $TM_{7,1}$ WGM at n_1 =3.4 and n_2= 2, 2.8, 3.1, and 3.17 obtained by FDTD simulation.

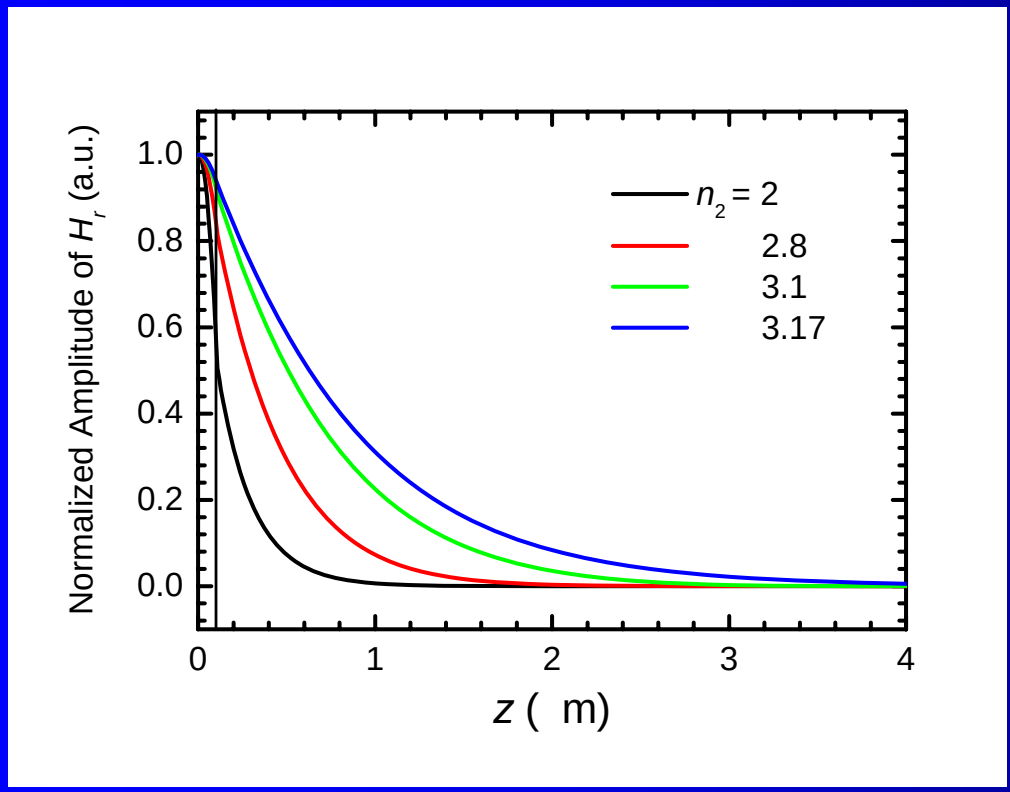

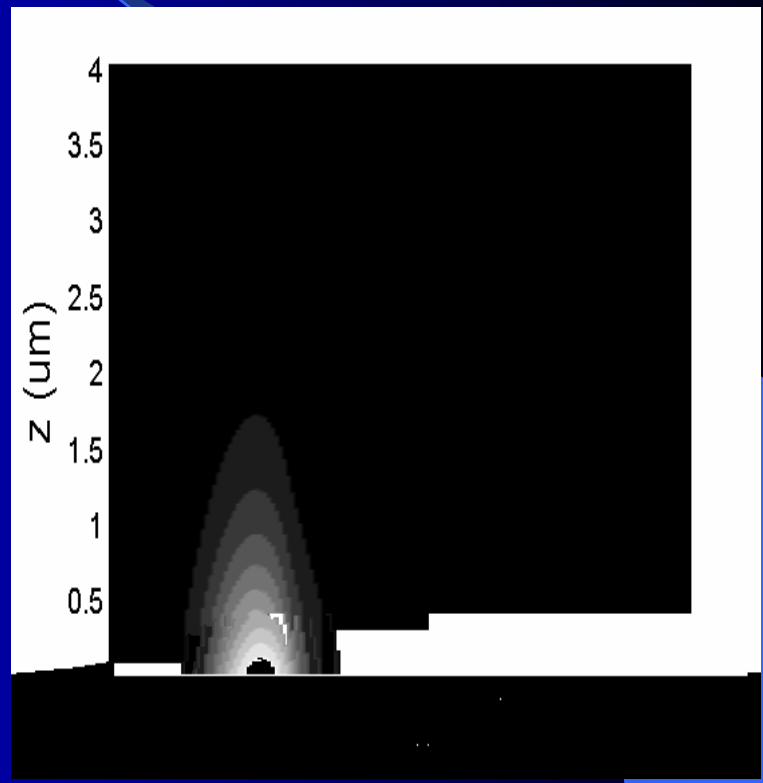

$r = 0.84R$

$n_2 = 3.17$

Mode wavelengths of WGMs and radiation modes for microcyliner with vertical refractive indices 3.4/3.17

R (m)	1.0	2.0	3.0	4.0	5.0	6.0
Mode index	9	21	33	45	58	70
λ -TM WGM (m)	1.658	1.589	1.584	1.586	1.565	1.574
λ -TE WGM (m)	1.532	1.533	1.548	1.560	1.546	1.558
λ (HE_{off}) (m)	1.641	1.572	1.566	1.569	1.548	1.556
λ (EH_{off}) (m)	1.511	1.511	1.526	1.539	1.527	1.537
Q (TE)	680	470	580	870	~10^4	~10^6

T. Baba et al, IEEE Photon. Technol. Lett., 9,

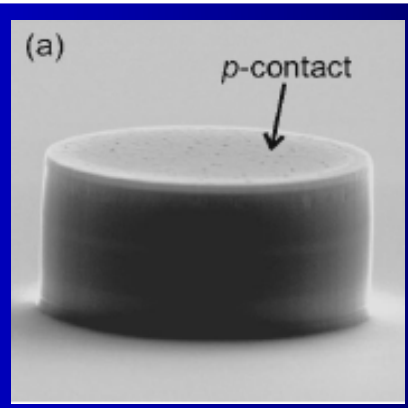

WG , TM WGM ,
, TE WGM ,
TE , ,
TM ,
WG .

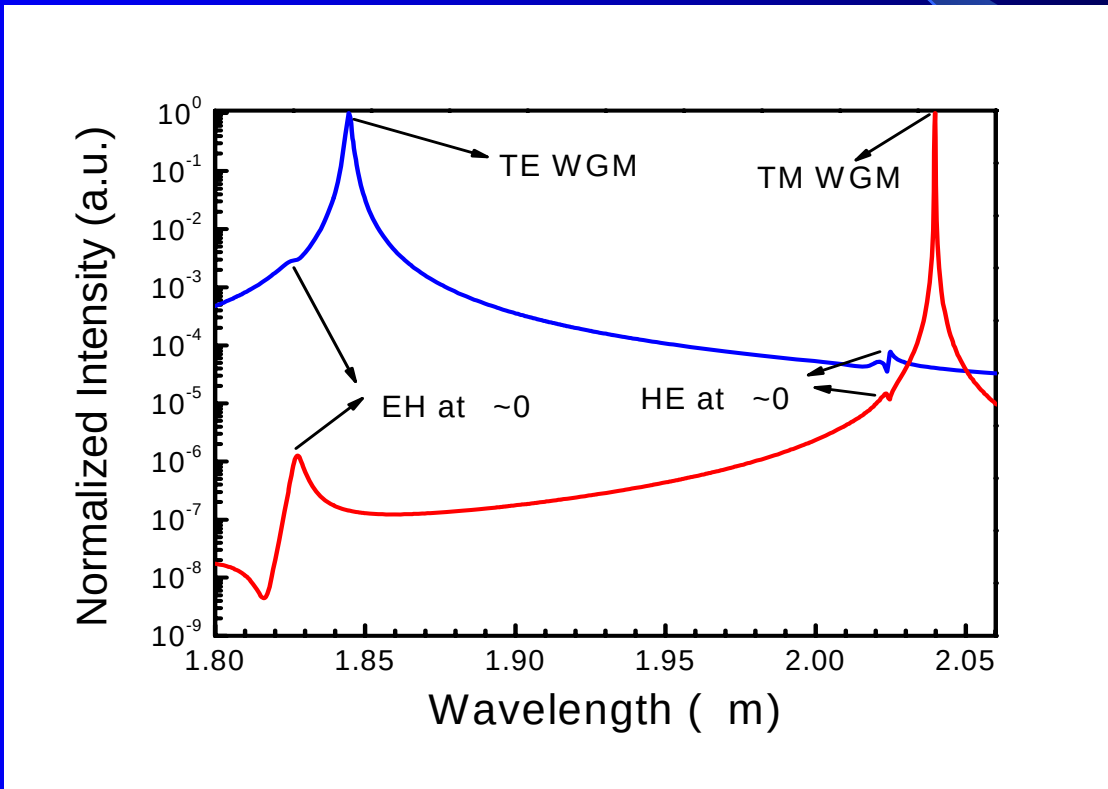

FDTD TE TM WGM EH HE .

TE WGM

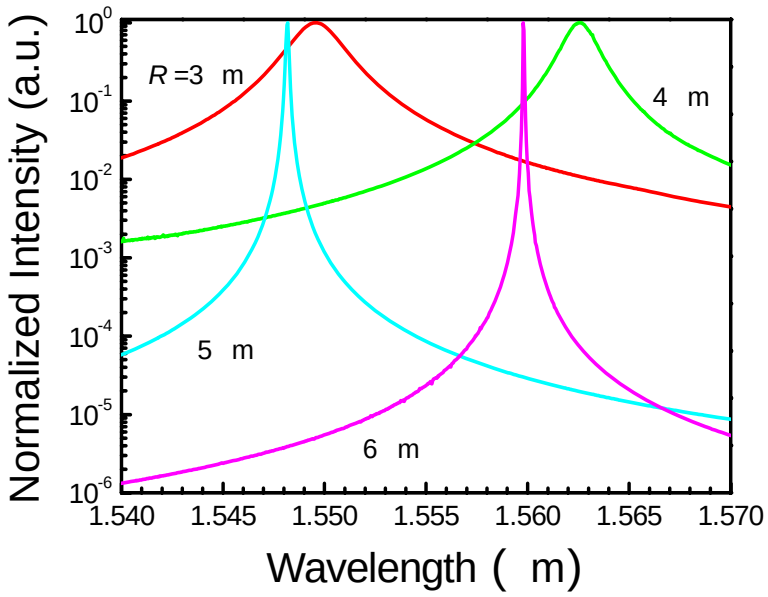

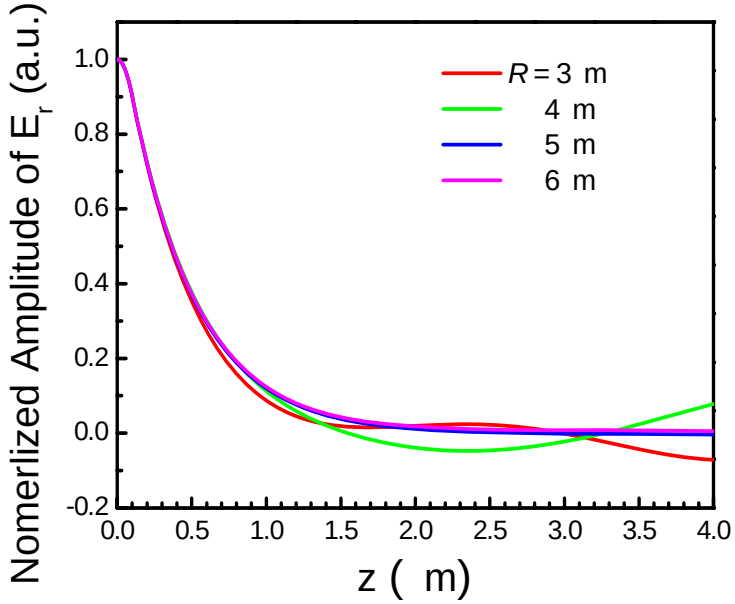

TM

,

TE 5~6 m, ,

.

Phys. Rev. A Vol.75 013817 (2007)

IEEE Photonics Technology Letters 19, 1831(2007)

五. 结论

(10-30)

TM 1

Thank You !